NATIONAL ENERGY TECHNOLOGY LABORATORY

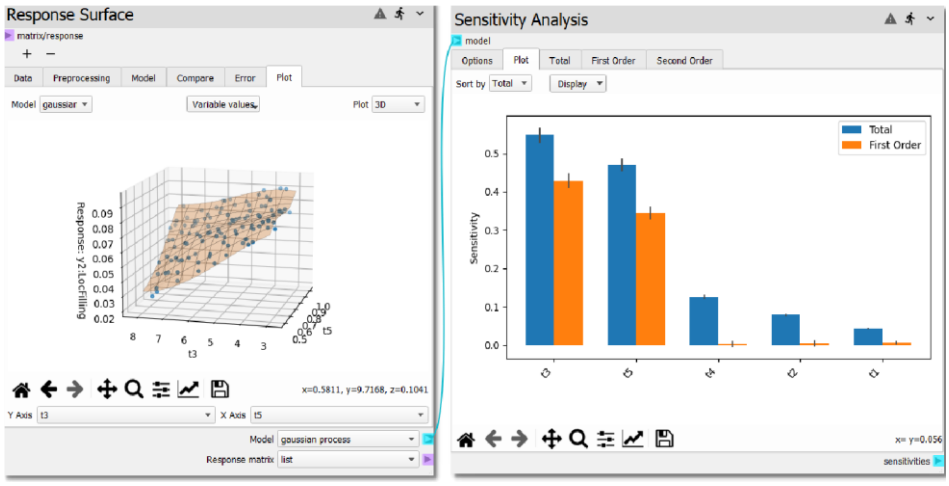

Sensitivity Analysis of MFiX-PIC Parameters Using Nodeworks, PSUADE, and DAKOTA

21 July 2021

U.S. DEPARTMENT OF ENERGY | NATIONAL ENERGY TECHNOLOGY LABORATORY

Office of Fossil Energy

DOE/NETL-2021/2652

Disclaimer

This project was funded by the United States Department of Energy, National Energy Technology Laboratory, in part, through a site support contract.

Cover Illustration: Screen shot of a workflow setup in Nodeworks demonstrating the construction and visualization of a Gaussian process surrogate model and using that surrogate model to evaluate the total and first order sensitivities of the MFiX particle-in-cell (PIC) model parameters.

Suggested Citation: Gel, A.; Weber, J.; Vaidheeswaran, A. *Sensitivity Analysis of MFiX-PIC Parameters Using Nodeworks, PSUADE, and DAKOTA*; DOE.NETL-2021.2652; NETL Technical Report Series; U.S. Department of Energy, National Energy Technology Laboratory: Morgantown, WV, 2021; p 52 . DOI:10.2172/1809024

Sensitivity Analysis of MFiX-PIC Parameters using Nodeworks, PSUADE, and DAKOTA

Aytekin Gel[1,3], Justin Weber[1], Avinash Vaidheeswaran[1,2]

[1] U.S. Department of Energy, National Energy Technology Laboratory, 3610 Collins Ferry Road, Morgantown, WV 26507

[2] NETL Support Contractor, 3610 Collins Ferry Road, Morgantown, WV 26505

[3] ALPEMI Consulting, L.L.C., 8205 S Priest Dr #13951, Tempe, AZ 85284

DOE/NETL-2021/2652

21 July 2021

NETL Contacts:

Jeff Dietiker, Mehrdad Shahnam, William Rogers, Co-Principal Investigators

William A. Rogers, Technical Portfolio Lead

Bryan Morreale, Executive Director, Research & Innovation Center

This page intentionally left blank.

Table of Contents

EXECUTIVE SUMMARY **1**

1. INTRODUCTION **2**

1.1 MOTIVATION 2

1.2 OUTLINE 2

2. OVERVIEW OF THE UQ SOFTWARE USED **5**

2.1 NODEWORKS 5

2.2 PSUADE 5

2.3 DAKOTA 6

2.4 COMPARISON OF UQ ANALYSIS CAPABILITIES 6

3. DEMONSTRATION CASES **8**

3.1 OVERVIEW OF DEMONSTRATION CASES CONSIDERED 8

3.2 CASE 1: GRAVITATIONAL PARTICLE SETTLING 8

3.3 CASE 2: FLUIDIZATION 10

3.4 CASE 3: CIRCULATING FLUIDIZED BED 11

4. SURROGATE MODELS CONSTRUCTED **13**

4.1 SIMULATION CAMPAIGNS DESIGNED TO CONSTRUCT SURROGATE MODELS 13

4.2 SURROGATE MODEL CONSTRUCTION 18

5. SENSITIVITYANALYSIS RESULTS **30**

5.1 SENSITIVITY ANALYSIS METHOD: SOBOL' SENSITIVITY INDICES 30

5.2 CASE 1: GRAVITATIONAL PARTICLE SETTLING 30

5.3 CASE 2: BUBBLING FLUIDIZED BED 31

5.4 CASE 3: CIRCULATING FLUIDIZED BED 33

6. CONCLUSIONS **36**

7. REFERENCES **37**

APPENDIX **A-1**

List of Figures

Figure 1: Schematic of particles settling in a dense medium. 9

Figure 2: Comparison of time evolution of shock fronts obtained using uncalibrated MFiX-DEM, MFiX-PIC, and MFiX-TFM simulations with the analytical solution..... 9

Figure 3: Schematic of Case 2 setup showing the computational domain and location of pressure ports..... 10

Figure 4: Instantaneous snapshots from fluidization experiments showing bed expansion for different U/U_{mf} (Vaidheeswaran et al., 2020). 11

Figure 5: Schematic of Case 3 setup showing the location of mass flow controllers..... 12

Figure 6: Snapshot of the experimental setup (left) and MFiX-DEM simulation (right) (Xu et al., 2018). 12

Figure 7: Scatter matrix plot of all input parameters and QoIs employed in simulation campaign for Case 1 using OLH design based 110 samples of simulations. 14

Figure 8: Scatter matrix plot of all input parameters and QoIs employed in simulation campaign for Case 2 using OLH design based 110 samples of simulations. 16

Figure 9: Scatter matrix plot of all input parameters and QoIs employed in simulation campaign for Case 3 using OLH design base (110 samples)..... 17

Figure 10: Nodes required for the Nodeworks workflow to construct a surrogate model after importing the simulation campaign dataset for QoI #2 (110 samples) into RSM node..... 19

Figure 11: Scaling of the input parameters under Preprocessing tab of the RSM node. 20

Figure 12: (Left) Quality assessment metrics displayed for the tested different surrogate models under Model tab. (Right) Visual comparison of the surrogate model quality assessment metric under Compare tab. 21

Figure 13: Scatter matrix plot showing the original simulation campaign (110 samples shown in black filled circles) and the new 10 samples (red filled circles) used for comparing the surrogate model results from PSUADE, DAKOTA, and Nodeworks. 22

Figure 14: Comparison of quadratic polynomial based surrogate model computed for Case 1 QoI (y2:Location of filling shock) for the 10 new samples. 23

Figure 15: Comparison of results obtained for Case 1 QoI (y2:Location of filling shock) with the 10 evaluation samples from the Gaussian process surrogate model results from PSUADE, DAKOTA, and Nodeworks. 24

Figure 16: MSE of cross-validation at different alpha values. 25

Figure 17: Comparison of results obtained for Case 2 QoI #1 (y1:dP2) with the 10 evaluation samples from the surrogate model results from PSUADE, DAKOTA, and Nodeworks. 26

Figure 18: Comparison of results obtained for Case 2 QoI #2 (y2:dP3) the 10 evaluation samples from the surrogate model results from PSUADE, DAKOTA, and Nodeworks. 26

List of Figures (cont.)

Figure 19: Comparison of results obtained for Case 3 QoI #1 (interface height in standpipe) with the 10 evaluation samples from the surrogate model results from PSUADE, DAKOTA, and Nodeworks..... 27

Figure 20: Comparison of results obtained for Case 3 QoI #2 (pressure drop across riser) with the 10 evaluation samples from the surrogate model results from PSUADE, DAKOTA, and Nodeworks..... 28

Figure 21: Comparison of results obtained for Case 3 QoI #3 (pressure drop across standpipe) with the 10 evaluation samples from the surrogate model results from PSUADE, DAKOTA, and Nodeworks..... 29

Figure 22: Comparison of Sobol' Total Indices for global sensitivity analysis results from Nodeworks, PSUADE, and DAKOTA with the same input deck provided for Case 1 QoI #1… 31

Figure 23: Comparison of Sobol' Total Indices for $y_1 : \Delta P_2$ based on the results from Nodeworks, PSUADE, and DAKOTA with the same input deck provided for Case 2 QoI # 1. 32

Figure 24: Comparison of Sobol' Total Indices for $y_2 : \Delta P_3$ based on the results from Nodeworks, PSUADE, and DAKOTA with the same input deck provided for Case 2 QoI # 2. 32

Figure 25: Comparison of Sobol' Total Indices for $y_3 : \Delta P_4$ based on the results from Nodeworks, PSUADE, and DAKOTA with the same input deck provided for Case 2 QoI # 3. 33

Figure 26: Comparison of Sobol' Total Indices for Case 3 QoI # 1 (y1: Interface height in standpipe) based on the results from Nodeworks, PSUADE, and DAKOTA with the same input deck provided..... 34

Figure 27: Comparison of Sobol' Total Indices for Case 3 QoI # 2 (y2: Pressure drop across riser) based on the results from Nodeworks, PSUADE, and DAKOTA with the same input deck provided..... 34

Figure 28: Comparison of Sobol' Total Indices for Case 3 QoI # 3 (y3: Pressure drop across standpipe) based on the results from Nodeworks, PSUADE, and DAKOTA with the same input deck provided..... 35

List of Tables

Table 1: Comparison of Features Implemented in Nodeworks, PSUADE, and DAKOTA under Several UQ Capabilities..... 7

Table 2: List of Input Parameter Abbreviations, Descriptions, Lower, and Upper Bounds Values Considered in the Simulation Campaign for Case 1..... 14

Table 3: List of Input Parameter Abbreviations, Descriptions, Lower, and Upper Bounds Values Considered in the Simulation Campaign for Case 2..... 15

Table 4: List of Input Parameter Abbreviations, Descriptions, Lower, and Upper Bounds Values Considered in the Simulation Campaign for Case 3..... 17

Acronyms and Abbreviations

Term	Description
ASCII	American Standard Code for Information Interchange
CFB	Circulating fluidized bed
CFD	Computational fluid dynamics
CSV	Comma separated values text file
DEM	Discrete element method
DOE	U.S. Department of Energy
GPM	Gaussian Process Model
GUI	Graphical user interface
HDPE	High-density polyethylene
LGPL	GNU Lesser General Public License
MC	Monte Carlo
MCMC	Markov Chain Monte Carlo
MFiX	Multiphase Flow with Interphase eXchanges
MFiX-DEM	MFiX discrete element method solver
MFiX-PIC	MFiX particle-in-cell solver
MFiX-TFM	MFiX two-fluid model solver
MOAT	Morris One-At-A-Time
MSE	Mean Squared Error
NETL	National Energy Technology Laboratory
OLH	Optimal Latin Hypercube
PCE	Polynomial Chaos Expansion
PIC	Particle-in-cell
QoI	Quantities of Interest (a.k.a. response variable)
RBF	Radial Basis Functions
SLPM	Standard liter per minute
SSE	Sum of Squared estimate of Errors
TFM	Two-fluid model
UQ	Uncertainty quantification
VVUQ	Verification, validation and uncertainty quantification

List of Symbols

Symbol	Description
R^2 or R-squared	Goodness-of-fit measure for linear regression models (-)
θ_1 or Theta1 or t1:P_0	Pressure linear scale factor, P_0 (Pa)
θ_2 or Theta2 or t2:beta	Volume fraction exponential scale factor, β (-)
θ_3 or Theta3 or t3:StatWeight	Statistical Weight, W_p (-)
θ_4 or Theta4 or t4:ep_g*	Void fraction at maximal close packing, ϵ_g^* (-)
θ_5 or Theta5 or t5:VelfacCoeff	Solids slip velocity scale factor, α (-)
x_1 or x1	Initial solids concentration, ϵ_{s0} (-)
y_1: *LocSettling*	QoI # 1 for Case 1: Location of Settling Shock (m)
y_2: *LocFilling*	QoI # 2 for Case 1: Location of Filling Shock (m)
y_3: *EpgFirstCell*	QoI # 3 for Case 1: Void fraction at the first cell (-)
y_1:ΔP_2 or y_1:dP2	QoI # 1 for Case 2: Pressure drop between 1 and 2 (Pa)
y_2:ΔP_3 or y_1:dP3	QoI # 2 for Case 2: Pressure drop between 2 and 3 (Pa)
y_3:ΔP_4 or y_1:dP4	QoI # 3 for Case 2: Pressure drop between 3 and 4 (Pa)
y_4:ΔP_5 or y_4:dP5	QoI # 4 for Case 2: Pressure drop between 1 and 4 (Pa)
y_1:h_standpipe	QoI # 1 for Case 3: Interface height in standpipe (m)
y_2:dP_riser	QoI # 2 for Case 3: Pressure drop across riser (Pa)
y_3:dP_standpipe	QoI # 3 for Case 3: Pressure drop across standpipe (Pa)
t	time (s)

Due to font constraints in plotting software, alternate abbreviated forms of the symbols were used for parameters and quantities of interest as shown in the above List of Symbols.

Acknowledgments

This work was performed in support of the U.S. Department of Energy's (DOE) Fossil Energy Crosscutting Technology Research Program. The research was executed through the National Energy Technology Laboratory's (NETL) Research and Innovation Center's CFD for Advanced Reactor Design (CARD) Field Work Proposal.

The authors wish to acknowledge Dr. William A. Rogers for programmatic guidance, direction, and strong support to carry out this research. The authors also would like to thank Dr. Charles Tong of Lawrence Livermore National Laboratory for the support he provided in using PSUADE. The support obtained from DAKOTA Development members Dr. Laura P. Swiler for Polynomial Chaos Extension based sensitivity analysis with DAKOTA, Dr. Brian M. Adams and Dr. John Adam Stephens for other DAKOTA setup and usage related questions are also acknowledged.

EXECUTIVE SUMMARY

The increasing adoption of engineering designs based on modeling and simulation necessitates assessment of credibility of the numerical results. Uncertainty quantification (UQ) has thus become a major thrust area in the field of computational sciences, especially when applied in engineering research and development. UQ is often considered at the intersection of multidisciplinary domains such as statistics, probability theory, computer sciences, and engineering, which necessitates expertise in these domains collectively. Although there are a number of different software tools where UQ methods have been implemented and offer users to perform UQ analysis in a structured way, the expertise required to use these software toolkits effectively is no less than the expertise required to understand the methods.

To enable an easier adoption of UQ methodologies, a graphical workflow based software has been developed at the U.S. Department of Energy's (DOE) National Energy Technology Laboratory (NETL) as part of the ongoing Verification, Validation and Uncertainty Quantification (VVUQ) initiatives. Nodeworks (https://mfix.netl.doe.gov/nodeworks) is an open-source toolset written in Python. It was developed for enabling users to tackle challenging tasks like non-intrusive UQ analysis, optimization, or supervised machine learning through visually constructed workflows. Nodeworks utilizes the existing optimization and UQ libraries in Python's ecosystem such as SciPy, SALib, Scikit-Learn, etc., and embeds them in specialized nodes. Users can perform non-intrusive UQ analysis or optimization through the connection of available analysis nodes or user-defined custom nodes to construct a workflow.

The study presented in this report was aimed to demonstrate UQ analysis performed not only with Nodeworks, but also two other well-established UQ software tools from the U.S. DOE's National Laboratories (PSUADE from Lawrence Livermore National Laboratory and DAKOTA from Sandia National Laboratory). It is important to emphasize that the motivation of this study was not to determine the best UQ software, but to verify if the global sensitivity analyses from the end-to-end workflow in Nodeworks are consistent with the results of other two UQ software. The components of Nodeworks from Python's ecosystem have been tested as standalone libraries. However, an assessment study for the complete workflow targeting a specific UQ analysis has not been performed for Nodeworks. Hence, this study is expected to serve as an equivalent of solution verification for Nodeworks using other established UQ tools as reference solution. For this purpose, three distinct flow configurations (i.e., settling bed, bubbling fluidized, and circulating fluidized bed) have been used as representative multiphase flow problems of interest. The results of the systematic simulation campaigns performed in an earlier study using the particle-in-cell (PIC) approach in the Multiphase Flow with Interphase eXchanges (MFiX) suite of solvers (i.e., MFiX-PIC) was utilized. The same set of tabulated results was provided as input to the different UQ software for global sensitivity analysis. Results for the three cases indicate that based on the Sobol' Sensitivity Indices method the order of importance ranking determined by Nodeworks for the Sobol' Total Sensitivity Indices is consistent with PSUADE and DAKOTA in each case for the five model parameters considered. The input files for Nodeworks for the three cases are also shared through NETL's Gitlab repository for the reader interested in reproducibility and further analysis (See Section 1.2).

1. INTRODUCTION

1.1 MOTIVATION

Uncertainty quantification (UQ) is increasingly becoming a critical component of simulation-based engineering, where the credibility of the model predictions needs to be assessed with established methods, such as forward propagation of input uncertainties or global sensitivity analysis. Non-intrusive UQ techniques where the application software, such as a finite-volume discretization based fluid flow model, is treated as a black box and random drawing-based samples from model results are utilized to perform the analysis has been of particular interest (Gel et al., 2013a,b). These non-intrusive techniques allow for the use of existing and commercial software where significant development would be required to utilize intrusive UQ techniques. To support these types of analyses, various UQ software tools have been developed and are available both under commercial and open-source licensing.

The work presented here focuses on global sensitivity analysis methodology as part of the ongoing UQ efforts at the U.S. Department of Energy's (DOE) National Energy Technology Laboratory (NETL), and comparison of the sensitivity analysis results obtained from multiple UQ software tools (Nodeworks, PSUADE, and DAKOTA). The same dataset generated from the simulation campaign using the PIC (particle-in-cell) solver in the open-source software suite Multiphase Flow with Interphase eXchanges (MFiX) was provided as input to each UQ toolkit. Three distinct problems covering different flow regimes typically encountered were investigated: gravitational particle settling, fluidization, and a circulating fluidized bed.

In an earlier study by Vaidheeswaran et al. (2021) the sensitivities of five MFiX-PIC model parameters were analyzed through global sensitivity analysis using Nodeworks. This current work aims to establish a direct comparison of the sensitivity analysis results obtained from two additional UQ software packages (PSUADE and DAKOTA) by providing the same input deck to all three UQ packages and seeing if the same input variable ranking of importance is achieved. It is important to note that the aim is not to compare the capabilities of the UQ software to identify which one is the best, but to provide some sort of a solution verification process for Nodeworks by comparing against other established UQ capabilities, which have gone through their own verification processes. This study will serve as the documentation that demonstrates Nodeworks' several features are working as intended.

1.2 OUTLINE

This report is part of activities designed to document verification, validation, and uncertainty quantification studies for MFiX-PIC (NETL, 2021). However, the focus is primarily assessing the UQ capabilities of Nodeworks (NETL, 2020a,b; Weber et al., 2020), utilizing the results generated from MFiX-PIC simulations. Although Nodeworks can be operated as an independent tool, its tight integration with the MFiX suite of solvers enables users to perform various tasks with complicated workflows, such creating simulation campaigns with a statistical design of experiments, sensitivity analysis, or optimization. The layout of this report is arranged to help the reader, with the first section providing a brief background of the UQ software utilized (Section 2). Then a high-level overview of the three demonstration cases selected for the sensitivity analysis comparison is provided in Section 3. Some details on the surrogate models constructed to be utilized during sensitivity analysis in lieu of the actual MFiX-PIC simulations are presented

in Section 4. Finally, the comparison of the sensitivity results obtained from three UQ toolkits for the three distinct demonstration cases are presented in Section 5.

Several UQ methods and UQ software toolkits were used in the analysis presented in this report. Associated files for Nodeworks are also shared through NETL's Gitlab for the reader who is interested in reproducing the findings provided that same software setup is employed. However, it is important to note that the intent of this report does not include teaching the reader the theoretical underpinnings of statistical analysis as it relates to surrogate model construction or sensitivity analysis, nor how to use associated software. In each of the relevant sections, additional references are provided to direct the user to more comprehensive guidance, if required.

Workflow for the Global Sensitivity Analysis Employed in this Study

The workflow outlined below was followed to perform the Sobol' Sensitivity Indices based global sensitivity analysis presented in this study.

1. Identify the model parameters to be investigated for sensitivity analysis, and determine the lower and upper bounds for each of these parameters to be used.
2. Plan a simulation campaign with the aid of statistical design of experiments principles that will enable the construction of a data-fitted surrogate model. The surrogate model should adequately characterize the relationship between model parameters considered as input and the response variables (a.k.a. quantities of interest (QoI) or output). This step is crucial when the simulations are expensive or time consuming to perform as the sensitivity analysis process requires thousands of function evaluations of the QoI to be performed cheaply.
3. Post-process the simulation campaign results and compile an American Standard Code for Information Interchange (ASCII) based file as a tabulated dataset consisting of the design of experiments for the model parameters and the corresponding QoIs from the simulation campaign results. This should be prepared in Comma Separated Values (CSV) or plain ASCII format for importing into UQ software easily.
4. Utilize UQ software (Nodeworks, PSUADE, and DAKOTA) to import the datasets and perform the global sensitivity analysis employing Sobol' Sensitivity Indices method, which is classified under variance decomposition methods (Sobol', 2001, Trucano et al., 2006). Note that the surrogate model constructed is used to perform the evaluations of the QoI required for Sobol' Sensitivity Indices computations, in lieu of actual MFiX-PIC simulations for each instance. Hence, the performance of the surrogate model to accurately represent the parameter space needs to be carefully assessed prior to the optimization step with measures such as adjusted R^2 or cross-validation error assessment. Doing so ensures the error introduced by the surrogate is minimized.
5. Plot and compare the computed Sobol' Total Sensitivity Indices from Nodeworks, PSUADE, and DAKOTA for the corresponding QoI in each case considered. It is important to note that the same simulation campaign based dataset was provided as input to all UQ software.

This report also includes a separate data management and repository section (Appendix A). There, the user is given information necessary to replicate the global sensitivity analysis described for Nodeworks only as the objective of this study was to conduct a solution verification study for Nodeworks. For example, results in this report rely on specific versions and libraries of Nodeworks, Python, PSUADE, and DAKOTA. If the user trying to reproduce the data in this work does not apply the same versions of the employed software and pathway to solution, it should not be surprising if exact results are not replicated especially due to randomness involved in the use of particular data sampling techniques (like Latin Hypercube). However, the user should expect to see consistent results, provided their solution process is similarly sound.

Note: The results presented in this document and shared through Gitlab were based on MFiX-PIC version 20.1 simulations. The authors have become aware of a bug in the MFiX-PIC solver that affects the results from simulation campaigns presented. As the objective of this work was to demonstrate and compare the sensitivity analysis with PSUADE, DAKOTA, and Nodeworks for any given input dataset (i.e., simulation campaign inputs and quantities of interest), no further revisions were implemented. However, the readers are warned about the potential differences should the reader use MFiX-PIC other than version 20.1 to replicate the simulation campaigns.

The files used in the analyses performed with Nodeworks are available within NETL's Gitlab environment, which is accessible through the following URL:

https://mfix.netl.doe.gov/gitlab/quality-assurance/pic-sensitivity-study.git

The repository is publicly accessible at the time of the writing of this report.

The purpose of the repository is two-fold: to have the information necessary to fully replicate this study, and to provide the reader with a baseline to begin their own exploration of global sensitivity analysis utilizing a surrogate model constructed from a systemically designed simulation campaign. Note, however, that there is a *clear expectation* that a person accessing this repository has pre-existing knowledge of how to use the Nodeworks software, which is the primary focus of this study. For other software used as comparison for Nodeworks, the reader is advised to review the respective websites and user manuals of the relevant UQ software.

2. OVERVIEW OF THE UQ SOFTWARE USED

Three open-source UQ software tools were employed in this study: Nodeworks (NETL, 2020a,b, Weber et al., 2020), PSUADE (Tong, 2010; Tong, 2020), and DAKOTA (Adams, 2008, Adams et al., 2009). Although all three UQ software tools have nearly the same non-intrusive UQ analysis options available, there are some differences in terms of implementation of the UQ methods and also additional advanced UQ features, such as Bayesian Calibration, multifidelity surrogate models, etc. Table 1 aims to provide a high level overview of similarities and differences between these three UQ software tools under three UQ analysis capabilities. Hence, it is not a comprehensive comparison.

2.1 NODEWORKS

Nodeworks, developed at NETL, is an open-source graphical programming interface library and workflow framework where users can add, delete, and connect nodes to create customized visual workflows (NETL, 2020a,b; Weber et al., 2020). Nodes perform prescribed operations on data whose results are then passed to other nodes using connections (or edges). The library was specifically developed in the Python programming language to remain flexible, portable, and take advantage of all the libraries available in the Python ecosystem. It can support a wide variety of applications and contains several collections of default nodes to assist deployment of commonly used workflows quickly, even for novice users. Users can also create and add custom nodes for specific applications. This work leverages a collection of nodes known as the Surrogate Modeling and Analysis Toolset, which was developed to implement workflows that construct and use data-fitted surrogate models or response surfaces. The Surrogate Modeling and Analysis Toolset provides access to specialized nodes including optimization, sensitivity analysis, and forward propagation of uncertainty.

Additionally, Nodeworks is directly embedded into MFiX's graphical user interface (GUI), thus allowing Nodeworks to create MFiX input decks with parametrically varying inputs directly. This allows for simple setup and management of simulation campaigns. Similarly, Nodeworks can be employed by other modeling software to create workflows with ease.

2.2 PSUADE

PSUADE is an open-source UQ software toolkit developed at the Lawrence Livermore National Laboratory by Dr. Charles Tong (Tong, 2010) and released under GNU Lesser General Public License (LGPL) since 2007. The name of the software, PSUADE, comes from the acronym for Problem Solving Environment for Uncertainty Analysis and Design Exploration. The program supports a variety of non-intrusive UQ analysis methods where the simulation application can be treated as "black-box" code. Subsequently, many UQ analysis tasks can be performed by sampling the black-box directly or through a data-fitted surrogate model constructed from the computational model. The software offers a diverse range of sampling methods to enable users to perform simulation campaigns with the objective of constructing an adequate data-fitted surrogate model (a.k.a. response surface model, meta-model). The user can perform both basic uncertainty analysis such as forward propagation of uncertainties and more complex analysis like mixed aleatory-epistemic uncertainty analysis. PSUADE has a built-in statistical calibration capability (i.e., Bayesian calibration with Markov Chain Monte Carlo (MCMC)). However, deterministic calibration requires user-defined supporting code to incorporate residual

evaluations. PSUADE is written in C++ and operates primarily as a command line based software, which may be an impediment to new users. Additional details on the capabilities of PSUADE can be found in https://computing.llnl.gov/projects/psuade/software (Tong, 2020).

2.3 DAKOTA

DAKOTA is an open-source software toolkit developed at the Sandia National Laboratory and distributed under LGPL (Adams, 2008, Adams et al., 2009). The acronym DAKOTA stands for Design Analysis Kit for Optimization and Terascale Applications. This general-purpose software toolkit is used to perform systems analysis and design on high performance computers. DAKOTA includes algorithms for design optimization, uncertainty quantification, parameter estimation, design of experiments, and sensitivity analysis, as well as a range of parallel computing and simulation interfacing services. These capabilities may be used independently or as components within advanced strategies such as surrogate-based optimization, mixed integer nonlinear programming, or optimization under uncertainty.

2.4 COMPARISON OF UQ ANALYSIS CAPABILITIES

It is difficult to make a direct comparison between the three UQ software. There have been several studies that attempted to identify the key features of available UQ software under several dimensions, such as Simpson et al. (2008) which presented a table showing the available capabilities for metamodeling and optimization in the commercially available software. Another study by the U.S. DOE's Pacific Northwest National Laboratory (Lin et al., 2012) aimed to survey the available UQ methods and then carried out a systematic evaluation of these methods implemented in ten UQ software identified, which included PSUADE and DAKOTA.

In the current study, Nodeworks version 20.2.0, PSUADE version 2.0, and DAKOTA version 6.13 were employed.

For additional information on the theoretical foundations and usage of these UQ software, the reader is referred to the resources in the references section for each software (NETL, 2020; Weber et al., 2020; Tong, 2010; Tong, 2020; Adams, 2008; Adams et al., 2009, 2015; Adams and Hough, 2012).

Table 1: Comparison of Features Implemented in Nodeworks, PSUADE, and DAKOTA under Several UQ Capabilities

	Nodeworks	PSUADE	DAKOTA
Sampling Methods			
(i) Classical Design of Experiments	Factorial, Central Composite Design	Factorial, Central Composite Design, Box-Benhken	Factorial, Central Composite Design, Box-Benhken
(ii) Space Filling Designs	Latin Hypercube, Monte-Carlo	Latin Hypercube, quasi-MC, Orthogonal arrays	Latin Hypercube, Monte-Carlo, Orthogonal arrays
Data-fitted Surrogate Models	Polynomial Regression, Gaussian Process Model (GPM), Radial Basis Functions (RBF), multilayer perceptron, support vector machine, decisions tree, random forest, gradient boosting, MARS, PyTorch	Polynomial Regression, Kriging, GPM, RBF	Polynomial Regression, Kriging, GPM, RBF
Sensitivity Analysis Methods	Sobol' Sensitivity Indices, Morris One-At-A-Time (MOAT), Fourier Amplitude Sensitivity Test (FAST), Delta Moment-Independent Measure	Sobol' Sensitivity Indices, MOAT	Sobol' Sensitivity Indices, MOAT via PSUADE interface

3. DEMONSTRATION CASES

3.1 OVERVIEW OF DEMONSTRATION CASES CONSIDERED

This report is part of series of studies on sensitivity analysis and calibration of MFiX-PIC that aims to utilize three industrial applications that span a wide range of flow regimes that is typically encountered. In particular, the studies/cases are particle settling, a fluidized bed, and a circulating fluidized bed..

3.2 CASE 1: GRAVITATIONAL PARTICLE SETTLING

The problem of particles settling under gravity in a dense medium has an analytical solution. This means that a well-controlled experiment would give exactly the same result as a hand calculation. From a calibration standpoint, this implies that there is no worry of added experimental error when evaluating any hypothetical physical set-up. Any hand-calculation for the solution is *the truth*. This indicates that the question of error moves entirely to the surrogate model generated from the simulation campaign.

The setup, borrowed from Vaidheeswaran et.al. (2020b), is described in Figure 1. The computational domain considered is 0.02 m (x-direction) × 0.02 m (z-direction) × 1 m (y-direction). Uniform grid sizes of 4 mm were used in the x- and z- directions, while a grid size of 2 mm was used in the y-direction. The duration of each simulation was 1 s, and a constant time-step size of 5e-4 s was used.

Once the simulation begins, two concentration (kinematic) shocks evolve. The first originates from the top of particle bed and corresponds to settling, while the other originates from the bottom and corresponds to filling. The location of the filling shock (y_2) is the quantity of interest (QoI) considered in this study. Its analytical solution is given by:

$$y_2(t) = -t\left(\frac{\epsilon_s^*\epsilon_g^* u_r^* - \epsilon_{s0}\epsilon_{g0}u_{r0}}{\epsilon_s^* - \epsilon_{s0}}\right) \tag{1}$$

where ϵ_s^* and ϵ_g^* are volume fraction of solids-phase and gas-phase at close packing. ϵ_{s0} and ϵ_{g0} are initial volume fractions. u_r^* and u_{r0} represent relative velocities calculated using close packing and initial conditions, respectively. The filling shock propagates upward when a lower region is fully packed by solids. Properly predicting the filling shock may correspond well with other simulations where solids concentration is high and particle motion is relatively slow. Previously, Vaidheeswaran et al. (2020b) used this case to compare results from MFiX-PIC, MFiX-TFM (two-fluid model), and MFiX-DEM (discrete element method) simulations as shown in Figure 2. Plots compare time evolution of concentration fronts from the three models with the analytical solution when $\epsilon_{s0} = 0.15$.

The location of settling shock (y_1) is another QoI post-processed from the simulations. This shock propagates in the direction of gravity, and corresponds to the transition between homogeneously distributed solids with concentration ϵ_{s0} and a dilute region where $\epsilon_s = 0$. The analytical solution for y_1 is given by,

$$y_1(t) = x_0 - t\,(\epsilon_{g0} u_{r0}) \tag{2}$$

Average void fraction at the first cell location (y_3) is the final QoI post-processed from simulations. However, both y_1 and y_3 are not considered in the current study. Using Equation 1, a standalone dataset was generated at 21 different x_1 settings where x_1 is equivalent to ϵ_{s0}, the initial solids concentration. Note that it is this dataset, consisting of 21 samples, that is used in lieu of experimental data required for deterministic calibration.

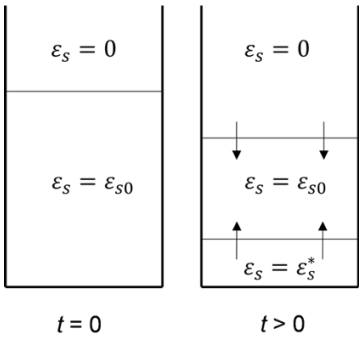

Figure 1: Schematic of particles settling in a dense medium.

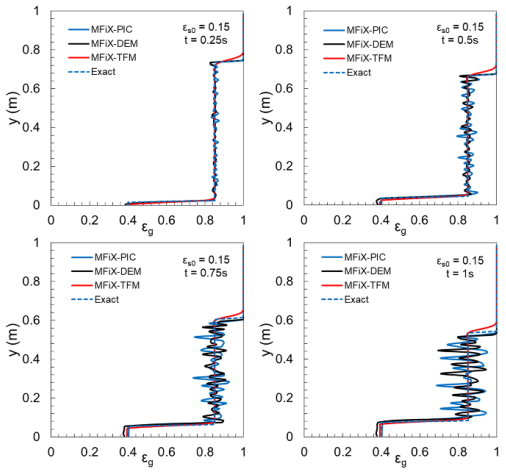

Figure 2: Comparison of time evolution of shock fronts obtained using uncalibrated MFiX-DEM, MFiX-PIC, and MFiX-TFM simulations with the analytical solution.

3.3 CASE 2: FLUIDIZATION

The case of bubbling fluidization corresponds to the study of Vaidheeswaran et al. (2020a) and Vaidheeswaran and Rowan (2020). Glass particles having density and Sauter mean diameter of 2510 kg/m^3 and 332 μm classified under Group B based on Geldart's criterion (Geldart, 1973) were used. Three different geometries and five different flow conditions were analyzed, and one particular setting was selected for the current study as shown in Figure 3. The internal diameter of the cylinder is 6.35 cm. Several measurement ports are located along the axis to measure differential pressure, of which $\Delta P_2 = P_1 - P_2$, $\Delta P_3 = P_2 - P_3$, and $\Delta P_4 = P_3 - P_4$ are used as QoIs (y_1, y_2, and y_3, respectively). y_1 and y_2 are useful in understanding the sensitivity of model parameters under dense flow conditions while at higher velocities compared to the settling case. y_3 contains the transition between dense and dilute regions where particles constantly engage and disengage, and it remains to be determined if the existing closure models in PIC are capable of handling such transitions. Figure 4 shows instantaneous snapshots of bed expansion at different U/U_{mf}, where the red line indicates the height determined by the image processing technique used in Vaidheeswaran et al. (2020a).

The computational domain consists of a single cylinder, whose bottom end is a mass inflow boundary, where a value of U = 0.234 m/s is specified corresponding to $U/U_{mf} = 2.97$. A pressure outflow boundary condition is used at the top, while the walls are treated as no-slip boundaries. Glass particles are filled up to a height of 15.24 cm having a solids packing fraction of 0.6. A uniform grid 3.33 mm ×3.33 mm ×3.33 mm is used, and the simulations are run for a total duration of 50 s using a variable time step with a maximum value of 5E-4 s.

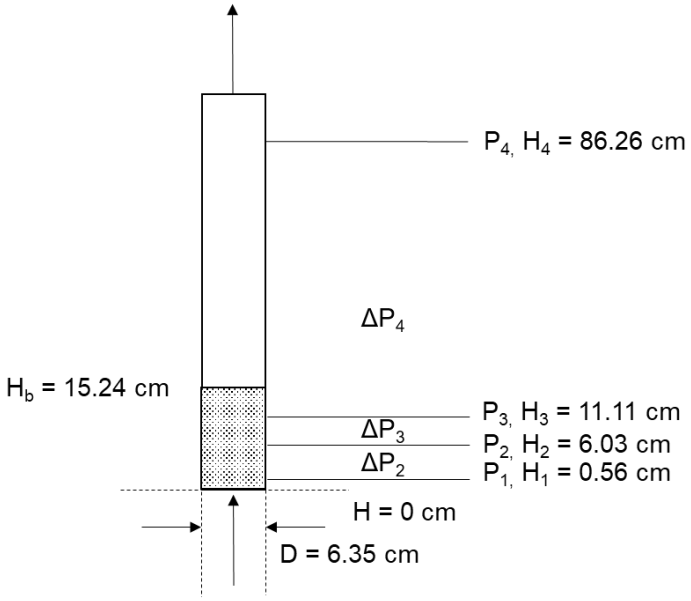

Figure 3: Schematic of Case 2 setup showing the computational domain and location of pressure ports.

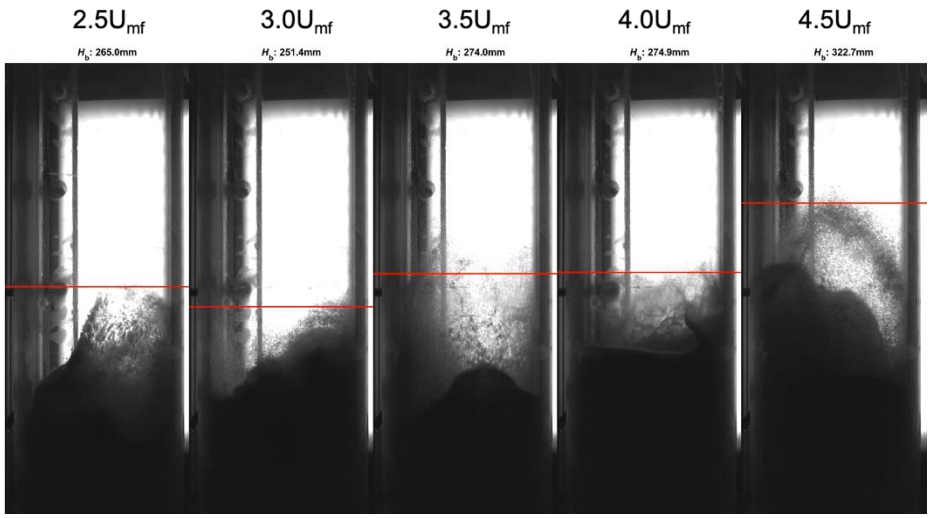

Figure 4: Instantaneous snapshots from fluidization experiments showing bed expansion for different U/U$_{mf}$ (Vaidheeswaran et al., 2020).

3.4 CASE 3: CIRCULATING FLUIDIZED BED

The setup of Xu et al. (2018) is used for analyzing the sensitivity of MFiX-PIC model parameters in a circulating fluidized bed (CFB). Figure 5 shows the schematic of the CFB configuration and Figure 6 shows comparison between experiments and numerical simulations using MFiX-DEM as reported by Xu et al. (2018). The CFB unit contained 350 g of high-density polyethylene (HDPE) particles having a Sauter mean diameter of 871 µm and a density of 863 kg/m^3 (grouped under Geldart B classification). Primary air was injected into the system using the flow controller FTC180 located below the riser. Move air was supplied using FTC135 and FTC115 at the top and bottom of the CFB return leg after the standpipe. The QoIs used in this study were interface height, pressure drop across riser, and pressure drop across standpipe (y_1, y_2, and y_3, respectively). In a sense, the dynamics in the standpipe are comparable to Case 1, where the particles motion is relatively slow. The move air flow past the standpipe ensures particles do not stagnate. Multiphase dynamics at the bottom of riser are comparable to the bubbling fluidized bed albeit at much higher air superficial velocity. The solids concentration is less compared to dense portions in Case 2.

The geometry and boundary conditions used in the simulation campaign were identical to the study of Xu et al. (2018). The grid size was set to 5 mm in all the directions. Flow rates from mass flow controllers FTC180, FTC135, and FTC115 used in this study were 300, 7, and 2.5 standard liter per minute (SLPM), respectively. Mass inflow boundary condition was specified at the bottom of the riser having a uniform velocity of 2.46 m/s. The computational fluid dynamics (CFD) calculations were performed over a duration of 45 s using a variable time step, with the maximum value set at 5e-4 s.

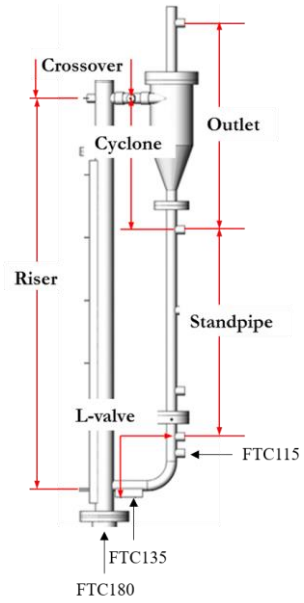

Figure 5: Schematic of Case 3 setup showing the location of mass flow controllers.

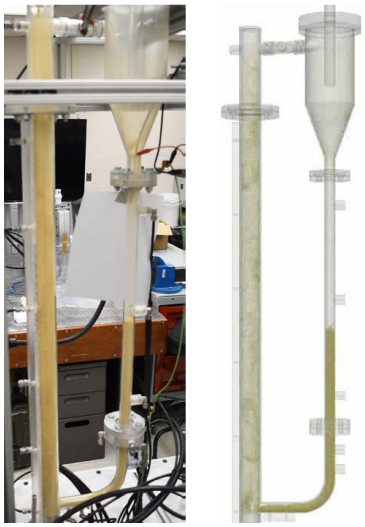

Figure 6: Snapshot of the experimental setup (left) and MFiX-DEM simulation (right) (Xu et al., 2018).

4. SURROGATE MODELS CONSTRUCTED

The non-intrusive uncertainty quantification method, such as the Sobol' Sensitivity Indices based global sensitivity analysis employed in this study, requires Monte Carlo simulations to be performed by randomly drawing different settings for each of the input parameters within their prescribed range and then computing the QoI for each sample. Although MFiX-PIC is substantially faster in time-to-solution when compared to the other MFiX suite solvers like MFiX-DEM or MFiX-TFM, performing Monte Carlo simulations by directly running MFiX-PIC at each new sample setting is not practical. Instead, a simulation campaign was systematically designed, using space filling techniques to have coverage for samples within each input parameter's lower and upper bounds. The sampling simulations in the campaign are carried out independently on a high-performance computing cluster. Then the simulation campaign results are compiled and utilized to construct a data-fitted surrogate model (a.k.a. response surface or meta-model) to characterize the relationship between the input parameters and QoIs (a.k.a. response variables) as reliably as possible. For additional detailed information on this important step, refer to Gel et al. (2013a, 2016).

Prior to presenting the Sobol' Sensitivity Indices based sensitivity analysis results, this section presents details on the simulation campaigns used to construct the surrogate models for each QoI in the three representative cases considered. It is important to note that, in non-intrusive UQ analysis surrogate model construction is one of the most time consuming and critical step as the quality of the constructed surrogate model directly affects the remaining UQ analysis.

4.1 SIMULATION CAMPAIGNS DESIGNED TO CONSTRUCT SURROGATE MODELS

Case 1: Particle Settling

An Optimal Latin Hypercube (OLH) sampling method implemented in Nodeworks was used to generate a sampling campaign for five MFiX-PIC input parameters. The first five were modeling parameters specific to MFiX-PIC, accessible to the user through keywords. These included: θ_1 : Pressure linear scale factor (P_0); θ_2 : Volume fraction exponential scale factor (β); θ_3 :Statistical Weight (W_p); θ_4 : Void fraction at maximal close packing$^{(\epsilon_g^*)}$; and θ_5 : Solids slip velocity scale factor (α). In the remainder of this report, abbreviated versions of the input parameter names have been used due to font issues in plotting software. Table 2 offers these abbreviations along with lower and upper bound values used for each model parameter in the simulation campaign. For example, anywhere t1:P_0 or t1 or Theta1 appears in this report, it is equivalent to θ_1:Pressure linear scale factor (P_0). It is noted that actual bounds generated at the end of Latin Hypercube sample generation are shown, which might be slightly different than the initially targeted bounds due to the randomness of the Latin Hypercube method (e.g., targeted upper bound for (P_0) was 20.0, but actual samples generated show a maximum value of 19.99).

Table 2: List of Input Parameter Abbreviations, Descriptions, Lower, and Upper Bounds Values Considered in the Simulation Campaign for Case 1

Symbol	Description	Min.	Max.
θ_1 or t1:P_0	Pressure linear scale factor, (P_0)	1.04	19.99
θ_2 or t2:beta	Volume fraction exponential scale factor, (β)	1.01	4.99
θ_3 or t3:StatWeight	Statistical Weight, (W_p)	3.04	7.96
θ_4 or t4:ep_g*	Void fraction at maximal close packing, (ϵ_g^*)	0.35	0.49
θ_5 or t5:VelfacCoeff	Solids slip velocity scale factor, (α)	0.5	0.99

The initial QoIs extracted from the simulation campaign were y_1:Location of Settling Shock; y_2:Location of Filling Shock; and y_3:Void fraction in the first cell nearest to the bottom of the experimental vessel. y_1 corresponds to the transition between dilute region of the settling bed and $\epsilon_g = 1$. It was of interest to determine the sensitivity of PIC parameters in regions having intermediate to dense solids concentration. Hence, y_1 was not considered in this study although MFiX-PIC computations were performed and the results were post-processed to compile this QoI. Also, y_3 has a single value (0.40) for all values of ϵ_{s0}, and it is not a suitable candidate for sensitivity analysis or calibration. y_2:Location of Filling Shock alone was considered as the QoI in Case 1. Note that in the remainder of this report, abbreviated versions of this QoI name might have been used such as y2:LocSettling corresponding to y_2 :Location of Filling Front or Shock due to font issues in plotting software.

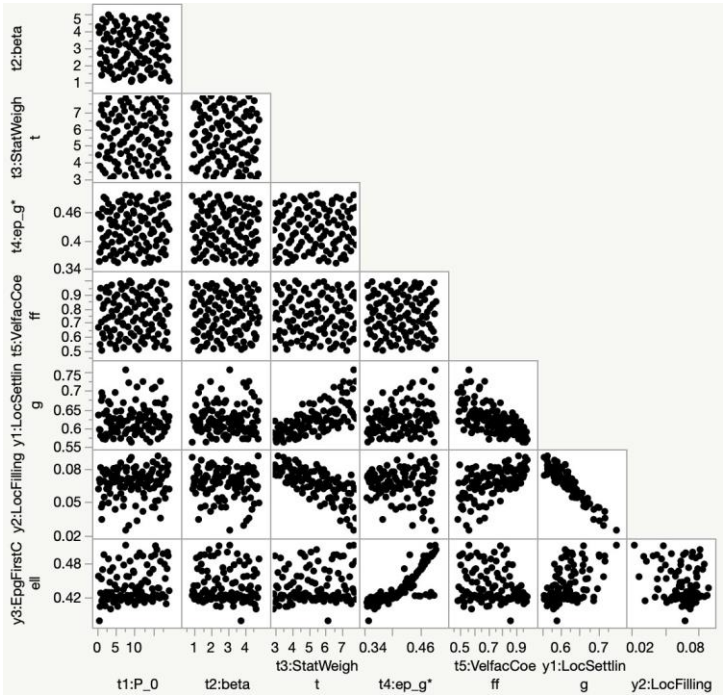

Figure 7: Scatter matrix plot of all input parameters and QoIs employed in simulation campaign for Case 1 using OLH design based 110 samples of simulations.

Figure 7 shows a scatter matrix plot of all input parameters and QoIs. This type of plot can be used to make a quick visual assessment of obvious correlations. For example, Figure 7 indicates that there appears to be a positive correlation between θ_4 : Void fraction at maximal close packing (ϵ_g^*) and y_3:Void fraction in the first cell nearest to the bottom of the experimental vessel; this evaluation is based on examining the block representing ($t4$ v. $y3$) as an independent graph and observing clustering of the samples to indicate an apparent positive correlation between the variables. Likewise, similar linear correlations, but inversely, can be seen in the block for $t3$ v. $y2$.

Refer to Appendix A.1 for the ASCII based dataset compiled at the end of the simulation campaign for Case 1 with 110 samples for the five input parameters and the three QoIs shown in Figure 7.

Case 2: Fluidization

Similar to the sampling method employed in Case 1, OLH method based sampling was employed for generating the simulation campaign for Case 2, which had the same five MFiX-PIC input parameters (θ_1,θ_2,θ_3,θ_4,θ_5), but with different lower and upper bounds for some of these input parameters as shown in Table 3. For example, θ_1:P_0 range was between 1.04 and 19.99 for Case 1, whereas the new upper bound for Case 2 was set as 99.83.

Figure 8 shows a scatter matrix plot of all input parameters and QoIs for Case 2, similar to that presented for Case 1 in Figure 7. The scatter plot matrix is useful to qualitatively identify the apparent correlated parameters such as θ_4:Void fraction at maximal close packing (ϵ_g^*) with the four QoIs ($y1 : \Delta P_2$, $y2 : \Delta P_3$, $y3 : \Delta P_4$) and $y4 : (\Delta P_5)$. The results for the first three QoIs are used in this analysis. The fourth QoI, $y4 : \Delta P_5$ is neglected because it is the difference in pressure between ports P_1 and P_4 in Figure 1, and is the sum of the other QoIs ($\Delta P_5 = \Delta P_2 + \Delta P_3 + \Delta P_4$).

Table 3: List of Input Parameter Abbreviations, Descriptions, Lower, and Upper Bounds Values Considered in the Simulation Campaign for Case 2

Symbol	Description	Min.	Max.
θ_1 or t1:P_0	Pressure linear scale factor, (P_0)	1.05	99.83
θ_2 or t2:beta	Volume fraction exponential scale factor, (β)	2.01	4.97
θ_3 or t3:StatWeight	Statistical Weight, (W_p)	10.61	99.78
θ_4 or t4:ep_g*	Void fraction at maximal close packing, (ϵ_g^*)	0.4	0.49
θ_5 or t5:VelfacCoeff	Solids slip velocity scale factor, (α)	0.85	0.98

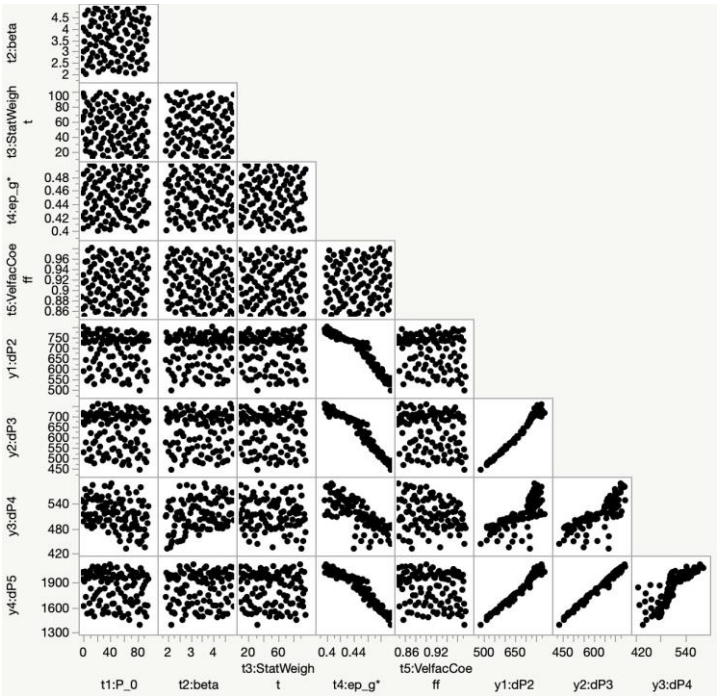

Figure 8: Scatter matrix plot of all input parameters and QoIs employed in simulation campaign for Case 2 using OLH design based 110 samples of simulations.

Refer to Appendix A.2 for the ASCII based dataset compiled at the end of the simulation campaign for Case 2 with 110 samples for five input parameters and four QoIs shown in Figure 8.

Case 3: Circulating Fluidized Bed

The same sampling method employed for the previous cases was used to construct the simulation campaign for Case 3 with 110 samples for the same 5 MFiX-PIC input parameters but some with different lower and upper bounds as shown in Table 4. The results for three QoIs were post-processed from the simulation campaign results: (i) Interface height in standpipe (y_1:h_standpipe), (ii) Pressure drop across riser(y_2:dP_riser), (iii) Pressure drop across standpipe (y_3:dP_standpipe).

Table 4: List of Input Parameter Abbreviations, Descriptions, Lower, and Upper Bounds Values Considered in the Simulation Campaign for Case 3

Symbol	Description	Min.	Max.
θ_1 or t1:P_0	Pressure linear scale factor, (P_0)	1.0	250
θ_2 or t2:beta	Volume fraction exponential scale factor, (β)	2.0	5.0
θ_3 or t3:StatWeight	Statistical Weight, (W_p)	10.32	206.34
θ_4 or t4:ep_g*	Void fraction at maximal close packing, (ϵ_g^*)	0.35	0.5
θ_5 or t5:VelfacCoeff	Solids slip velocity scale factor, (α)	0.85	0.98

Figure 9 shows the scatter matrix plot of all input parameters and QoIs considered for Case 3. The scatter matrix plot for this case does not show any particularly apparent correlations between input parameters and QoIs.

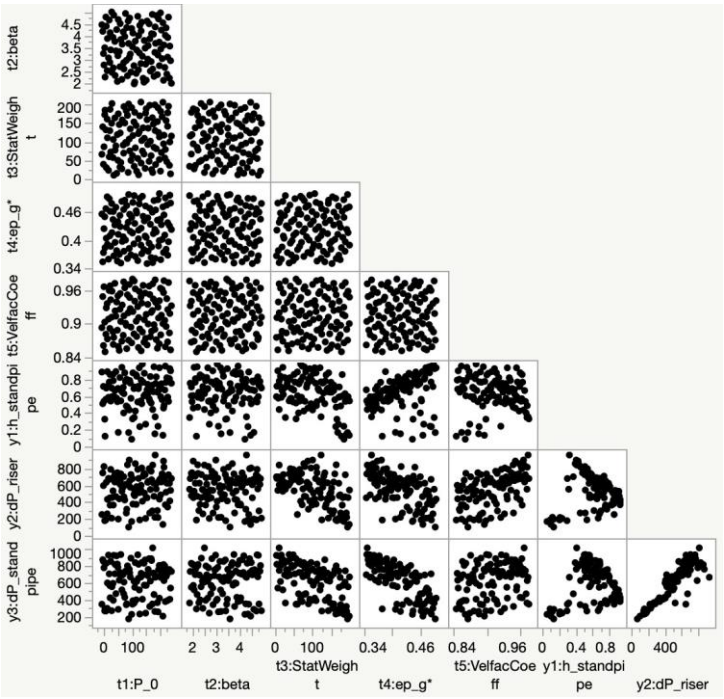

Figure 9: Scatter matrix plot of all input parameters and QoIs employed in simulation campaign for Case 3 using OLH design base (110 samples).

The reader is referred to Appendix A.3 for the ASCII based dataset compiled at the end of the simulation campaign for Case 3 with 110 samples for 5 input parameters and 3 QoIs shown in Figure 9.

4.2 SURROGATE MODEL CONSTRUCTION

After the simulation campaign results are post-processed, a tabulated dataset is compiled for each case to be provided as ASCII file based input to the three UQ libraries. To perform Sobol' Sensitivity Indices based global sensitivity analysis, a data-fitted surrogate model is constructed in lieu of the actual MFiX-PIC simulations for evaluating the QoIs at different settings of the five MFiX-PIC model input parameters. It is important to note that, the surrogate models are constructed to adequately characterize the relationship between input parameters and QoIs for the range of parameters. In other words, the constructed surrogate model is valid for the lower and upper bounds of each of the five MFiX-PIC model parameters determined when designing the simulation campaign to avoid running a new simulation each time. Hence, quality and adequacy of the surrogate model is important and needs to be adequately assessed. For a detailed discussion related to surrogate model construction, including adequacy assessments and error minimization, refer to Gel et al. (2013a,b, 2016, 2021).

As surrogate models are numerous and vary in form and function, for the purposes of this study a data-fitted surrogate model based on Gaussian Process Model (GPM) (Williams and Rasmussen, 2006) was determined to adequately characterize the relationship between the QoIs and input parameters for all three UQ programs with the same tabulated simulation campaign results provided as input. It is noted that if individually evaluated for the best data fitted surrogate model within each UQ software, one might be able to identify another surrogate model to be a better fit than GPM due to some differences in implementation of the surrogate model method. For example, radial basis function based surrogate model appeared to be giving slightly better fits for the QoI in Case2 when using Nodeworks. However, to establish a common comparison basis, the same surrogate model type, i.e., GPM was used across the board, although some implementation differences might yield to slight variations.

In the remainder of this section, the GPM based surrogate models constructed with Nodeworks is presented for each of the three cases, whereas for PSUADE and DAKOTA based surrogate models only the results are used directly for comparison basis as the scope of this study is not aimed to show how to construct a surrogate model with PSUADE and DAKOTA.

Nodeworks Based Surrogate Model for Case 1: Particle Settling

Figure 10 shows the workflow created to construct a surrogate model (a.k.a. response surface model) with Nodeworks. First, the Response Surface Model (RSM) node under Surrogate Modeling and Analysis nodes are added to a blank worksheet. Also, Parallel Coordinates Plot under matplotlib nodes option is added and connected to RSM node as shown in the figure by selecting "list" option in the Matrix Response port. The latter node is used to qualitatively visualize the simulation campaign dataset (i.e., 110 samples are shown as individual lines that pass through the six vertical axis corresponding to the five input parameters and one QoI) once it is imported into RSM node. The simulation campaign dataset, which is saved in CSV format, is imported through "Data" tab and selecting **Import** button. If the data is imported successfully, it is displayed in tabular format with parameter labels along the first line as shown in Figure 10. In the same figure, the Parallel Coordinates Plot node shown on the right side is displaying the dataset where each vertical column corresponds to one of the imported input parameters or QoI (usually the last column on right). This plot is helpful to identify outlier results qualitatively as such outliers could degrade the quality of the surrogate model constructed significantly and may

need to be investigated prior to better understand if they are non-physical results due to lack of convergence, meshing issues, or some other issue.

For additional information on how to construct a surrogate model within Nodeworks refer to (NETL, 2020; Weber, 2017, 2018).

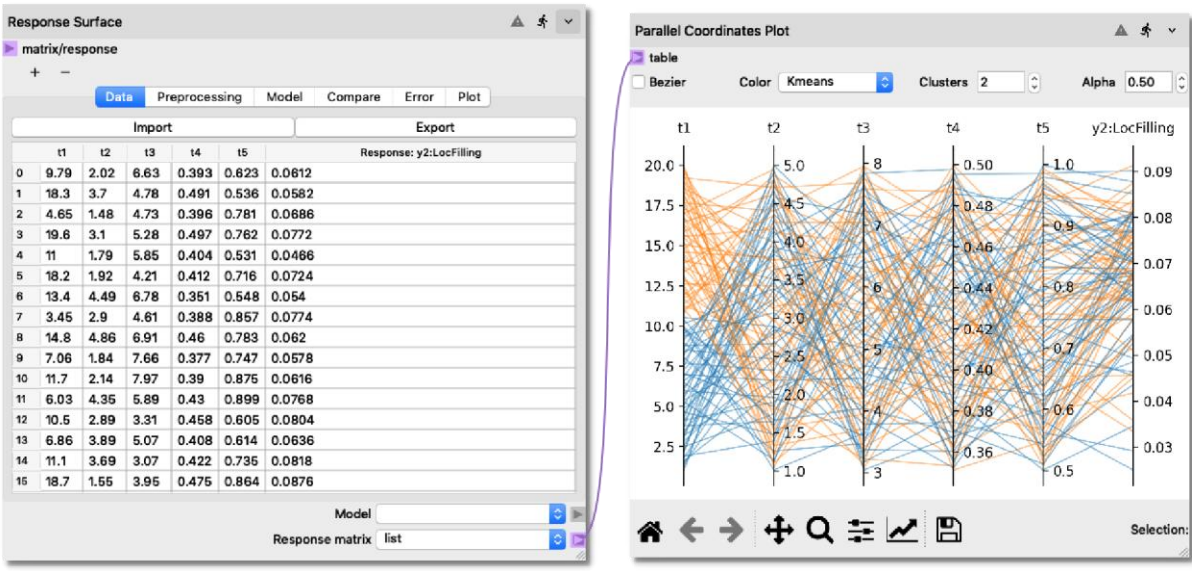

Figure 10: Nodes required for the Nodeworks workflow to construct a surrogate model after importing the simulation campaign dataset for QoI #2 (110 samples) into RSM node.

Figures 11–13 focus only on the RSM node shown in the above figure and demonstrate the pre-processing and model fitting steps, which are achieved through "Preprocessing" and "Model" tabs within the node, respectively. After the simulation campaign dataset is imported, a pre-processing step needs to be performed to scale the 110 samples of the five input parameters in the dataset to be between 0 and 1. Figure 11 shows the screenshot for the "Preprocessing" tab and selection of scale option to have all input parameters scaled to be between 0 and 1 values rather than their actual range. Some of the surrogate model methods have been determined to work better with scaled input parameters when constructing surrogate models.

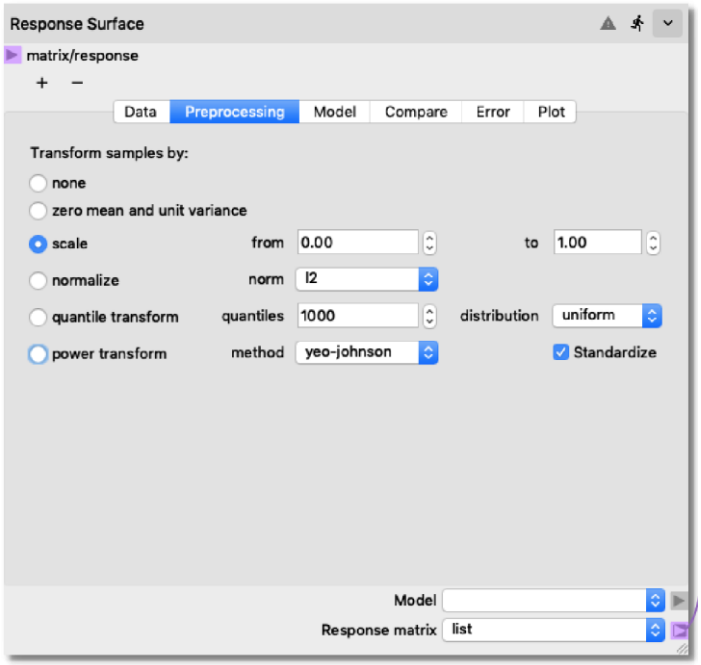

Figure 11: Scaling of the input parameters under Preprocessing tab of the RSM node.

Figure 12 (left) shows the surrogate model construction phase where the user selects the different types of surrogate models to be tested by clicking the checkmark in the left most column labeled **fit** to indicate which surrogate model methods to be included and constructed to identify the best data-fitted surrogate model for the given dataset. As shown in the figure, the following surrogate model methods have been selected and various quality metrics like Mean Squared Error (MSE), Sum of Squared estimate of Errors (SSE), R^2, etc., have been computed: (i) decision tree, (ii) radial basis function, (iii) Gaussian Process Model (a.k.a. GPM), (iv) gradient boosting, (v) random forest, (vi) polynomial, and (vii) support vector machine. After selection of the surrogate model options, the user may want to review each method to see if the default settings for the various parameters or hyperparameters used are satisfactory. For example, in Figure 12 (left) the hyperparameters for a GPM are shown when **gaussian process** line is clicked and highlighted. As discussed later, the value of **alpha** setting plays an important role for the quality of the GPM based surrogate model constructed with this dataset. After the review of the hyperparameters, **Refit Model(s)** button is clicked to initiate the process of surrogate mode construction for each of the selected methods, which may take some time and progress as shown in the title bar of the RSM node as green bar moving from left to right. After successful completion of the surrogate model fitting, the columns for MSE, SSE, R^2, L_inf, L_1, and L_2 will be populated with the computed corresponding metrics. The user can sort from lowest value to highest value by clicking the desired column header (e.g., Figure 12 shows surrogate models sorted from lowest value to highest for MSE column). A more visual comparison of the fitted surrogate models can be achieved through the **Compare** tab, which shows the comparison in terms of bar chart using the selected metric to rank from lowest to highest. For example, Figure 12 (right) shows comparison based on MSE metric. Details on evaluation of the surrogate model quality (e.g., performing a rigorous evaluation of the quality of the surrogate model constructed with cross-validation error assessment can be found in Nodeworks user manual and tutorials (NETL,

2020a,b). It is important to emphasize that if the analysis is reproduced using the files in Appendix A.1, there may be slightly different results than those shown in Figure 12 (left). This is due to the randomness involved in cross-validation assessment used in calculating the error metrics like MSE, SSE, R^2, etc.

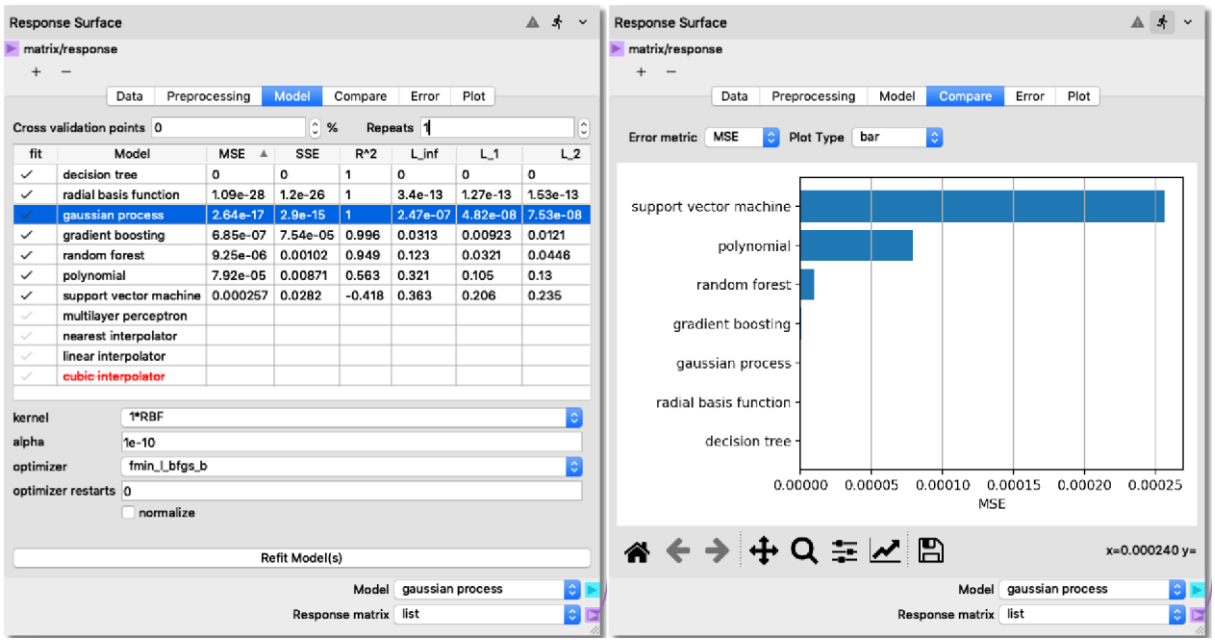

Figure 12: (Left) Quality assessment metrics displayed for the tested different surrogate models under Model tab. (Right) Visual comparison of the surrogate model quality assessment metric under Compare tab.

Once the user determines the best fitted surrogate model, it can be set under Model terminal port at the bottom right of RSM node for use in the analysis nodes downstream by connecting this terminal port to the next node such as Sensitivity Analysis node.

Comparison of the Surrogate Model Results for the Same Evaluation Points

Since surrogate models are designed to be abstract, allowing them to represent arbitrary responses, differences in implementation, hyper parameters, and even randomness can affect the resulting model. This makes it particularly hard to compare surrogate models across different software packages. However, since all the downstream analysis (such as global sensitivity study) relies on the surrogate model, it is important to understand the differences.

To illustrate the differences between UQ software employed, a study with 10 new sample points was carried out. The objective was to provide new unseen 10 sample points to all three UQ toolkits and perform evaluations of the QoI using the surrogate models constructed with each. Figure 13 shows the scatter plot matrix for the five model input parameters with 110 samples of the original simulation campaign (shown as black filled circles) and the new 10 samples used for comparing the surrogate model results (shown as red filled circles). The new 10 samples were generated with Latin Hypercube sampling method employing DAKOTA within the same lower and upper bounds of the model parameters. Instead of DAKOTA, PSUADE, or Nodeworks

could also have been used. The same set of samples were provided as input for surrogate model evaluations.

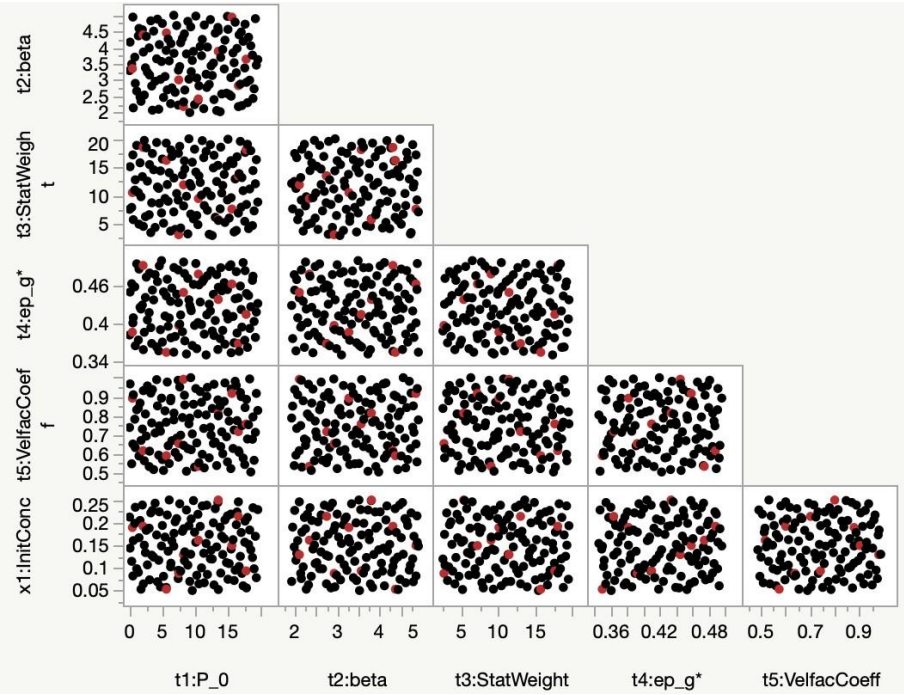

Figure 13: Scatter matrix plot showing the original simulation campaign (110 samples shown in black filled circles) and the new 10 samples (red filled circles) used for comparing the surrogate model results from PSUADE, DAKOTA, and Nodeworks.

To begin comparing the UQ tools, a simple cubic polynomial based surrogate model was fit with all three UQ libraries and evaluated with the 10 new samples. Specifically, for Nodeworks, the samples and response were normalized between 0 and 1, and the linear regressor was used with a tolerance of 1e-4. Figure 14 compares the evaluated 10 new samples between the three tools results in 0 % error, out to 8 decimal places. This provides validation that all three tools are reading the sample points, fitting surrogate models, and evaluating the surrogate models identically.

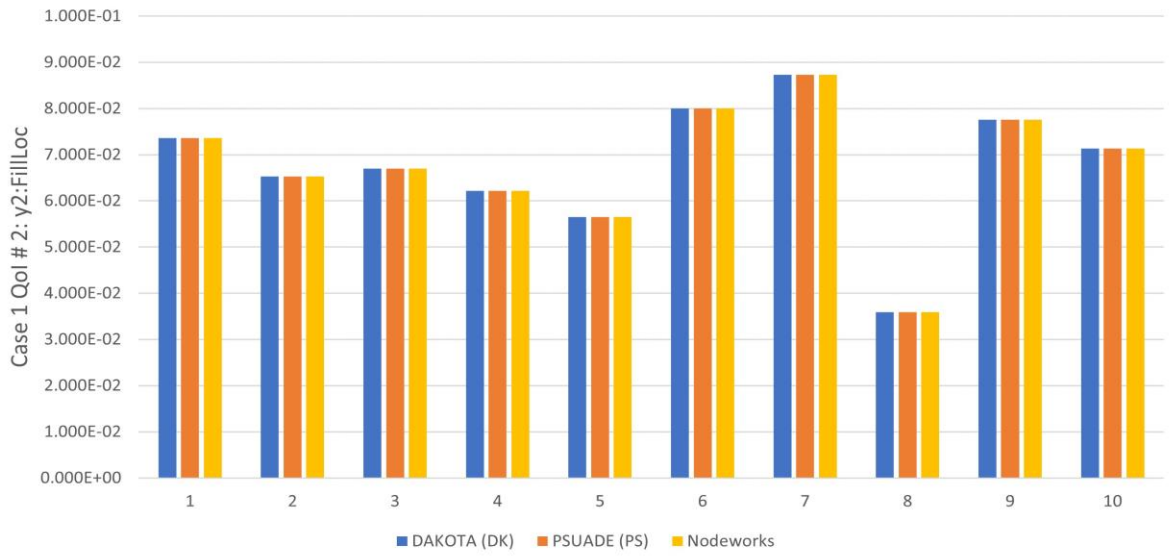

Figure 14: Comparison of quadratic polynomial based surrogate model computed for Case 1 QoI (y2:Location of filling shock) for the 10 new samples.

The same process was also performed with a GPM based surrogate model, which allows for many more degrees of freedom. It is currently unknown what specific Gaussian Process implementations are used in both DAKOTA and PSUADE. As a result, even with the same sample points, it is highly likely that the three UQ packages will produce different surrogate models due to differences in the implementations, pre-processing, and selection of hyperparameters.

Nodeworks uses scikit-learn for most of the surrogate models including Gaussian process. The scikit-learn documentation specifically references that the implementation is based on Algorithm 2.1 in Rasmussen et al. (2006). This allows users to prescribe kernels (also called "covariance functions") that are optimized during the fitting process. These kernels can drastically effect the resulting surrogate model. Nodeworks provides several default kernels as well as exposes other model parameters such as alpha (noise level in the targets).

Figure 15 shows a comparison of the QoI computed with the surrogate models constructed by DAKOTA, PSUADE, and Nodeworks for the 10 evaluation samples shown in Figure 13, which were highlighted with red filled circles. The maximum difference between PSUADE and DAKOTA based surrogate model results was 0.48 % and minimum difference was -0.33 %. A similar comparison was performed between PSUADE and Nodeworks based surrogate model results with the default settings, which shows 6.71 % and -21.28 % as the maximum and minimum difference, respectively. Nodeworks results are shown as two separate categories, i.e. untuned (labeled as "Nodeworks") and tuned (labeled as "Nodeworks Tuned"). Additional details about the tuning process are provided in the next section.

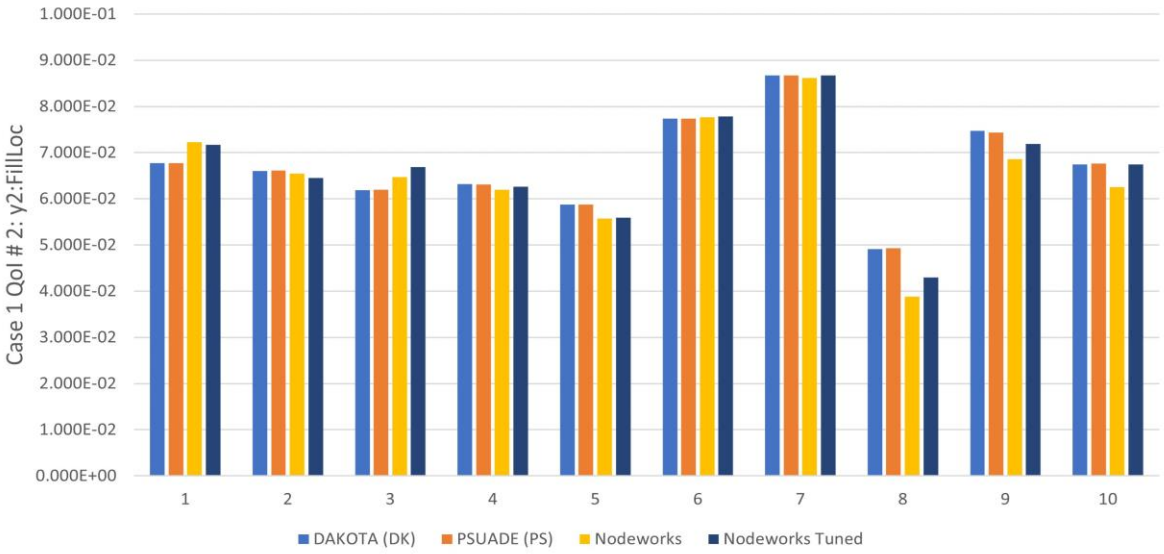

Figure 15: Comparison of results obtained for Case 1 QoI (y2:Location of filling shock) with the 10 evaluation samples from the Gaussian process surrogate model results from PSUADE, DAKOTA, and Nodeworks.

Hyperparameter Tuning in Nodeworks to Improve the Surrogate Model

Since some surrogate models, like the Gaussian process, have many options and hyperparameters, it is important to tune these so that the resulting response surface accurately characterizes the variability observed in the underlying data. For the Gaussian process in Nodeworks, the alpha parameter significantly affects the "smoothness" of the surface. The alpha value is added to the diagonal of the kernel matrix during fitting.

To optimize this alpha parameter, a series of alpha values were picked. At each value, the surrogate model was repeatedly fit 100 times and tested with a randomly drawn 10 % of the samples. This cross validation tests how well the surrogate model predicts the response values in-between the sample points. The MSE and the R-Squared (R^2) value at each alpha can then be compared, Figure 16. The smallest mean squared error was at an alpha of 0.05. At alpha values less than 0.001, the MSE is larger, suggesting over-fitting. Comparing this hand-tuned Nodeworks based surrogate model to the PSUADE model results in a maximum difference of 7.9 % and a minimum difference of -12.87 % compared to the untuned Nodeworks results, which reduces the under prediction in Nodeworks' surrogate model predictions nearly to half compared to PSUADE.

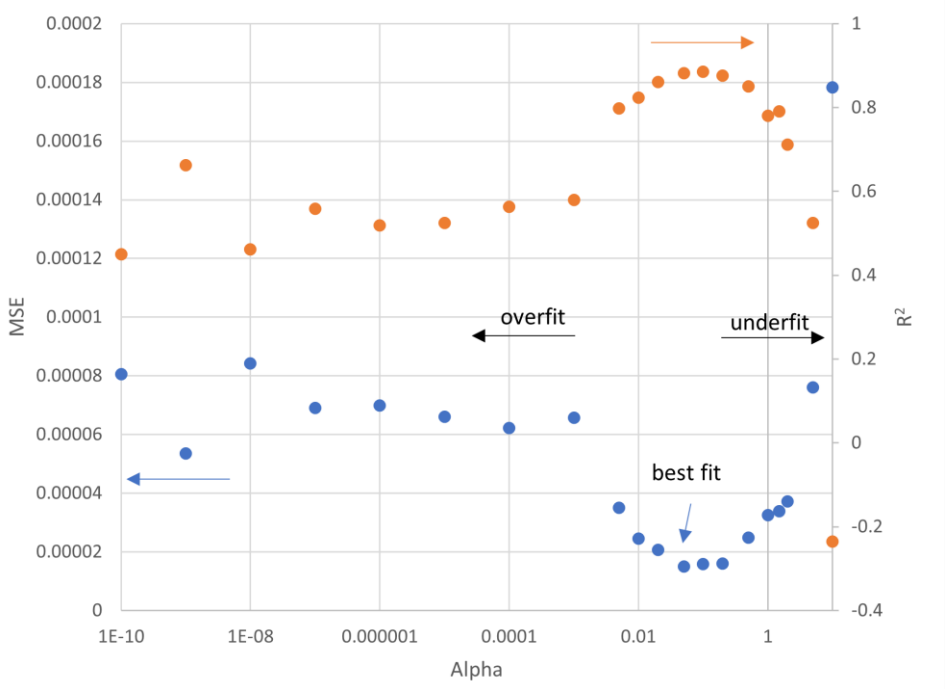

Figure 16: MSE of cross-validation at different alpha values.

Case 2: Fluidization

This case has three QoIs, which necessitated the construction of three distinct surrogate models for each QoI in UQ software. The same input, i.e., simulation campaign dataset consisting of the results from 110 samples of five model parameter settings and three QoIs were provided in a tabulated format.

An identical surrogate modeling process as described in Case 1 was followed here to construct the three Gausian process surrogate models need for further evaluations in Nodeworks. For brevity, a detailed description of the process is skipped. For further information and a copy of the Nodeworks workflow, see the gitlab repository mentioned in Section 1.2.

Comparison of the Surrogate Model Results for Same Evaluation Points

Similar to Case 1, 10 new sample points were generated to test and compare the trained surrogate models from the three packages.

For QoI#1: y1:dP2, all three packages predict similar response values, which is shown in Figure 17. The maximum difference between PSUADE and DAKOTA based surrogate model results was 0.42 % and minimum difference was -0.3 %. Similar comparison was performed between PSUADE and Nodeworks based surrogate model results with the default settings, which shows 3.38 % and -4.41 % as the maximum and minimum difference, respectively. The tuned Nodeworks surrogate model with an alpha of 1e-2 shows almost the same 3.38 % and -4.41 % maximum and minimum difference compared to PSUADE.

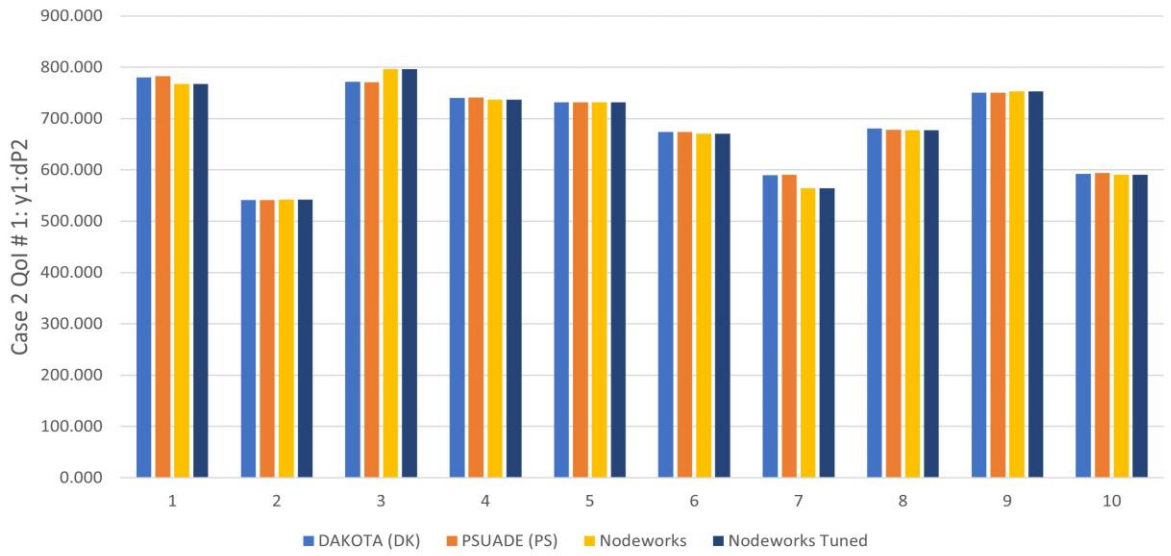

Figure 17: Comparison of results obtained for Case 2 QoI #1 (y1:dP2) with the 10 evaluation samples from the surrogate model results from PSUADE, DAKOTA, and Nodeworks.

For QoI#2: y2:dP3, all three packages also predict similar response values, as shown in Figure 18. The maximum difference between PSUADE and DAKOTA based surrogate model results was 0.19 % and minimum difference was -0.1 %. Similar comparison was performed between PSUADE and Nodeworks based surrogate model results with the default settings, which shows 7.54 % and -2.32 % as the maximum and minimum difference, respectively. The tuned Nodeworks surrogate model with an alpha of 1e-2 gets closer to PSUADE with a 3.56 % and -1.75 % maximum and minimum difference, respectively.

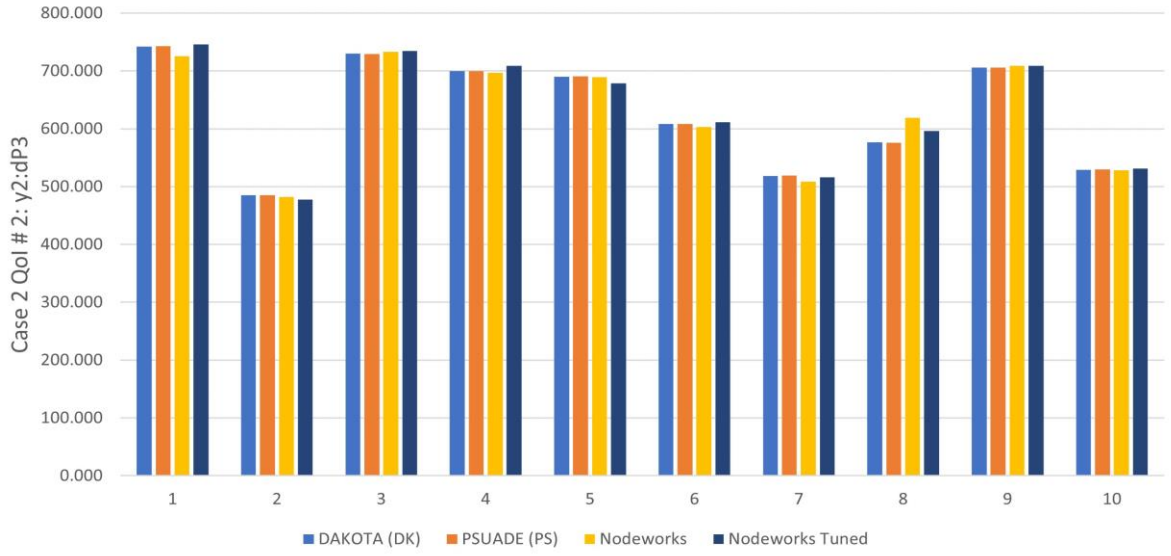

Figure 18: Comparison of results obtained for Case 2 QoI #2 (y2:dP3) the 10 evaluation samples from the surrogate model results from PSUADE, DAKOTA, and Nodeworks.

For the sake of brevity, the comparison for the last QoI is not shown.

Case 3: Circulating Fluidized Bed

This case has three QoIs. Hence, three distinct surrogate models for each QoI were constructed in the UQ software. The same input, i.e., simulation campaign dataset consisting of results from 110 samples of five model parameter settings and three QoIs were provided in a tabulated format.

An identical surrogate modeling process as described in Case 1 was followed here to construct the three Gaussian process surrogate models need for further evaluations in Nodeworks. For brevity, a detailed description of the process is skipped. For further information and a copy of the Nodeworks workflow, see the gitlab repository mentioned in Section 1.2.

Comparison of the Surrogate Model Results for Same Evaluation Points

Once again, 10 new sample points were generated to test and compare the trained surrogate models from the three packages.

For QoI#1: Interface height in standpipe, the three packages predict varying response values, as shown in Figure 19. The maximum difference between PSUADE and DAKOTA based surrogate model results was 75.93 % and minimum difference was -14.24 %. Similar comparison was performed between PSUADE and Nodeworks based surrogate model results with the default settings, which shows 201.29 % and -21.07 % as the maximum and minimum difference, respectively. The tuned Nodeworks surrogate model with an alpha of 1e-2 shows almost the same 198.45 % and -22.04 % maximum and minimum difference compared to PSUADE.

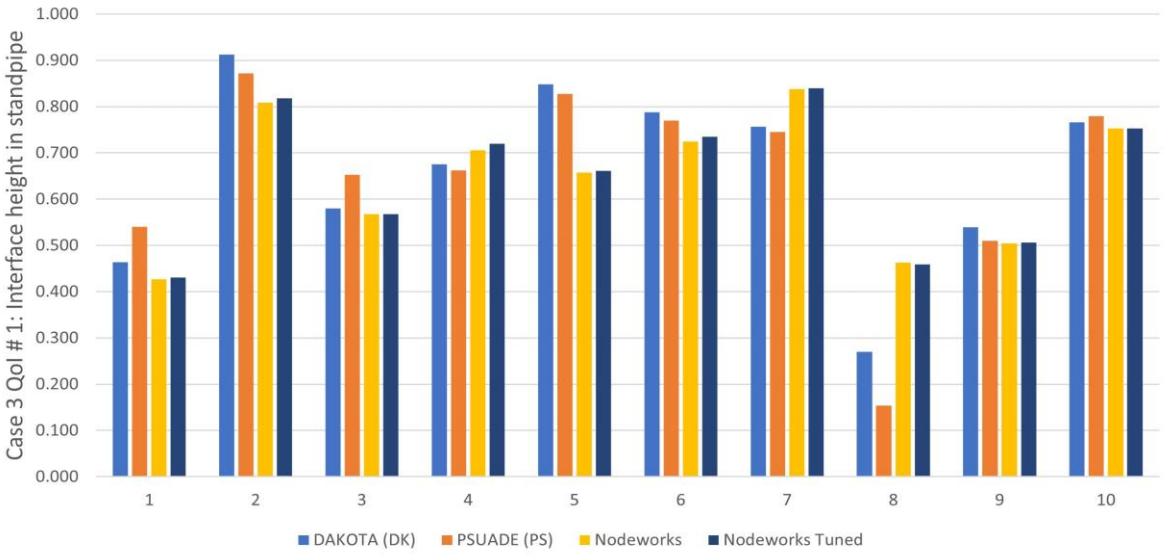

Figure 19: Comparison of results obtained for Case 3 QoI #1 (interface height in standpipe) with the 10 evaluation samples from the surrogate model results from PSUADE, DAKOTA, and Nodeworks.

For QoI#2: Pressure drop across riser, the three packages predict similar response values, as shown in Figure 20. The maximum difference between PSUADE and DAKOTA based surrogate model results was 0.74 % and minimum difference was -1.13 %. Similar comparison was performed between PSUADE and Nodeworks based surrogate model results with the default settings, which shows 21.35 % and -10.29 % as the maximum and minimum difference, respectively. The tuned Nodeworks surrogate model with an alpha of 1e-2 gets closer to PSUADE with 15.03 % and -3.09 % maximum and minimum difference.

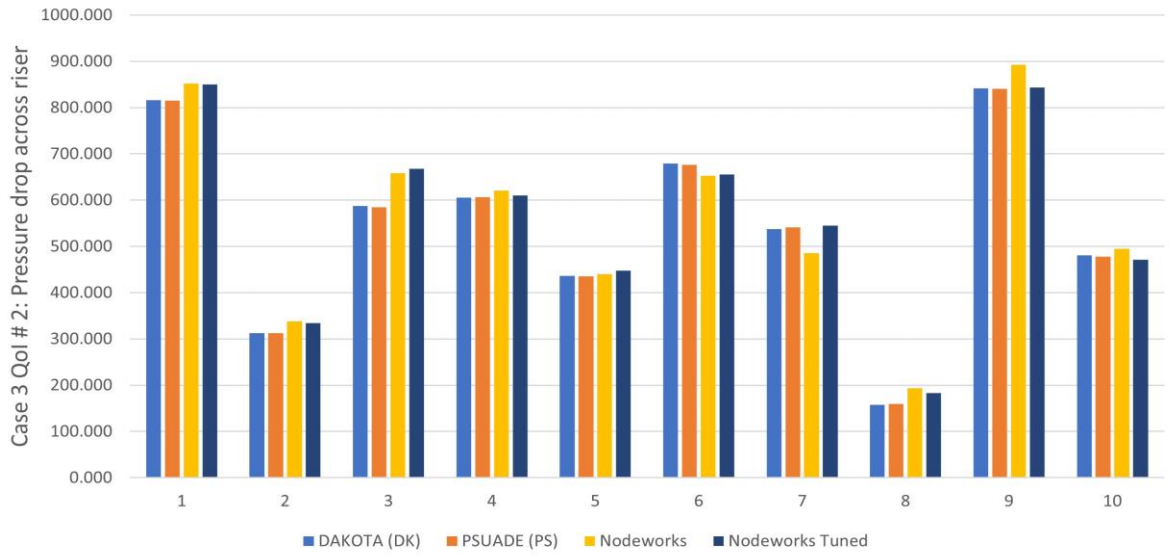

Figure 20: Comparison of results obtained for Case 3 QoI #2 (pressure drop across riser) with the 10 evaluation samples from the surrogate model results from PSUADE, DAKOTA, and Nodeworks.

For QoI#3: Pressure drop across standpipe, the three packages predict similar response values, as shown in Figure 21. The maximum difference between PSUADE and DAKOTA based surrogate model results was 1.6 % and minimum difference was -1.26 %. Similar comparison was performed between PSUADE and Nodeworks based surrogate model results with the default settings, which shows 22.39 % and -6.39 % as the maximum and minimum difference, respectively. The tuned Nodeworks surrogate model with an alpha of 1e-2 moves further away from PSUADE with 24.17 % and -6.23 % maximum and minimum difference.

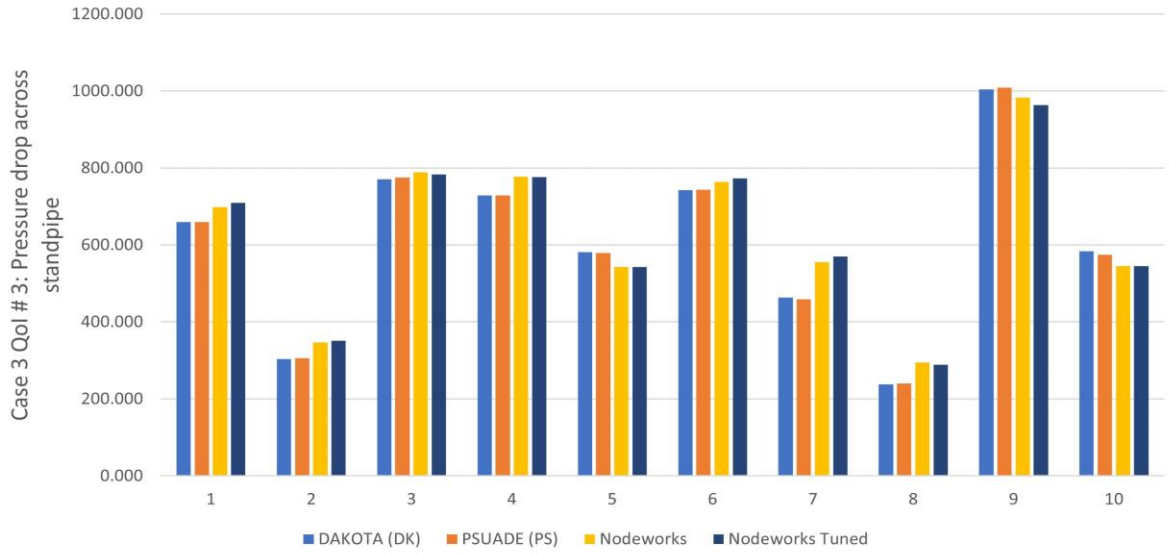

Figure 21: Comparison of results obtained for Case 3 QoI #3 (pressure drop across standpipe) with the 10 evaluation samples from the surrogate model results from PSUADE, DAKOTA, and Nodeworks.

5. SENSITIVITY ANALYSIS RESULTS

5.1 SENSITIVITY ANALYSIS METHOD: SOBOL' SENSITIVITY INDICES

Sensitivity analysis is one uncertainty quantification technique employed to address the important question: "Which input parameters have the most influence on the QoI?" The insight gained from sensitivity analysis can be critical. For example, it plays a key role during calibration, particularly when the number of input parameters exceeds three. The technique quantitatively determines the most influential parameters for each QoI, and can be used to focus the attention of experimentalists, especially when resources are limited.

The sensitivity analysis results in this report (Figures 22-28) were obtained using the Sobol' Sensitivity Indices based global sensitivity method, which is preferred for cases with non-linear response behavior. Sobol' Sensitivity Indices method can generate multiple indices such as Total Sensitivity Indices, First Order Sensitivity Indices, and Second Order Sensitivity Indices. In the current study, only Sobol' Total Sensitivity Indices were considered as they are more informative for the overall importance ranking. The data-fitted surrogate model was used to perform function evaluations for obtaining QoIs while calculating Sobol' Total Sensitivity Indices. The reader is referred to Sobol' (2001) and Iooss and Lemaître (2015) for additional information on the methodology and Gel et al. (2013a,b) for a demonstration with multiphase flow simulations. Additionally, a detailed sensitivity analysis study performed for the problems of interest with Nodeworks software can be found in Vaidheeswaran et al. (2021).

5.2 CASE 1: GRAVITATIONAL PARTICLE SETTLING

Global sensitivity analysis was performed using Sobol' Total Sensitivity Indices method, which is a variance decomposition based methodology implemented in all three UQ software considered. A previous sensitivity study was carried out in Nodeworks only (Vaidheeswaran et al., 2021). The current results might differ from the earlier results in (Vaidheeswaran et al., 2021) due to differences in the choice of surrogate model. Furthermore, a comparison between Sobol' Total Sensitivity Indices from Nodeworks, DAKOTA and PSUADE are shown which was not present in the earlier study.

Figure 22 shows the Sobol' Total Sensitivity Indices results, which assess the most influential parameters on the QoI, y_2:Location of Filling Shock. It is important to note that Total Indices take into account both main effects and their interaction effects on the QoI. Five different bars are shown for the results obtained from three different UQ software. For DAKOTA, in addition to the GPM based data-fitted surrogate model, Polynomial Chaos Expansion (PCE) based surrogate model is shown with "DAKOTA (PCE)" legend. Also results from Nodeworks are shown under two separate legends, first one shows the sensitivity indices obtained with GPM based surrogate models without any tuning using the default settings for GPM. The second one with the legend label of "Nodeworks (GPM Tuned)" shows the sensitivity indices obtained by employing a tuned GPM based data-fitted surrogate model. It is important to remember that the surrogate model plays a crucial role as it replaces the actual simulation code when performing the QoI evaluations required as part of the variance decomposition method employed (i.e. Sobol' Sensitivity Indices).

For the 110 sample simulation campaign results, $t3$:StatWeight appears to have the most pronounced effect on y_2:Location of Filling Shock, followed by $t5$:VelFacCoeff. The remaining parameters appear to exhibit substantially lower influence on the variability observed for QoI. Error bars shown in Nodeworks and PSUADE results are the confidence interval associated with 10000 and 100 sample bootstrapping for each parameter, respectively.

The differences observed in the magnitude of the Sobol' Total Indices can be attributed to the implementation differences of surrogate model (i.e., GPM) between three UQ software and the random drawings performed during the variance decomposition method based global sensitivity calculations. However, when the Sobol' Total Indices from each UQ software are individually considered, the results show that Nodeworks demonstrated the same ranking order (i.e., most influential parameters in their importance order: (Rank1) $t3$:StatWeight, (Rank2) $t5$:VelFacCoeff, (Rank 3) $t4$:ep_g*, (Rank 4) $t2$:beta, and (Rank 5) $t1$:P_0) with PSUADE and DAKOTA based results.

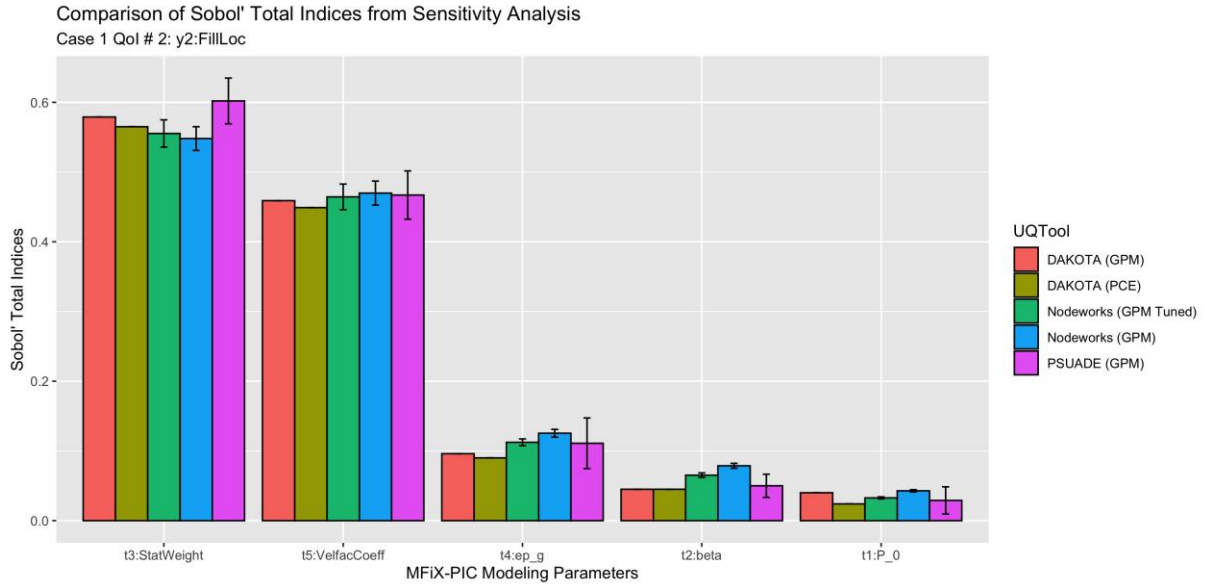

Figure 22: Comparison of Sobol' Total Indices for global sensitivity analysis results from Nodeworks, PSUADE, and DAKOTA with the same input deck provided for Case 1 QoI #1.

5.3 CASE 2: BUBBLING FLUIDIZED BED

Similar to the previous case, Sobol' Sensitivity Indices based global sensitivity analysis was performed using the 110 samples of the simulation campaign results obtained for the parameters listed in Table 3. As presented earlier, this case has three QoIs. Hence, Sobol' Sensitivity Indices analysis was performed for each QoI separately utilizing the data-fitted surrogate model constructed for each.

Figure 23 shows the Sobol' Total Sensitivity Indices results to assess the most influential parameters on the first QoI, $y_1 : \Delta P_2$. Sensitivity analysis results show $t4$:ep_g* to be distinctively

the most influential and dominant input parameter on $y_1 : \Delta P_2$. The error bar show the confidence interval associated with 100 sample bootstrapping for each parameter.

Confidence intervals do not show significant variability for any Sobol' Index estimated.

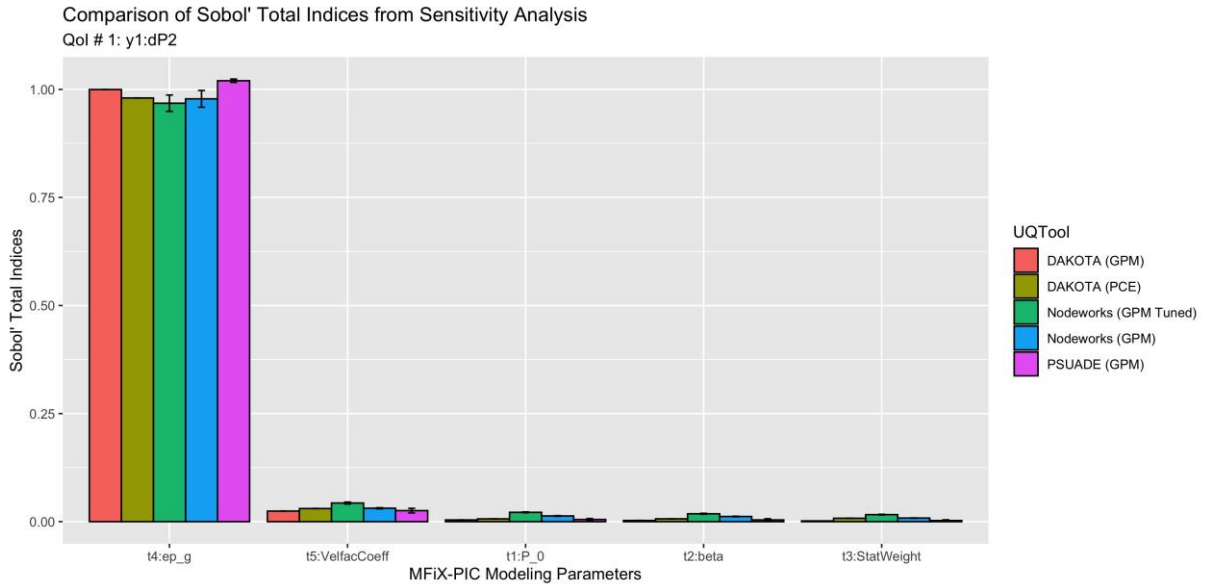

Figure 23: Comparison of Sobol' Total Indices for $y_1 : \Delta P_2$ based on the results from Nodeworks, PSUADE, and DAKOTA with the same input deck provided for Case 2 QoI # 1.

The same importance ranking is observed for the second QoI, $y_2 : \Delta P_3$ as shown in Figure 24.

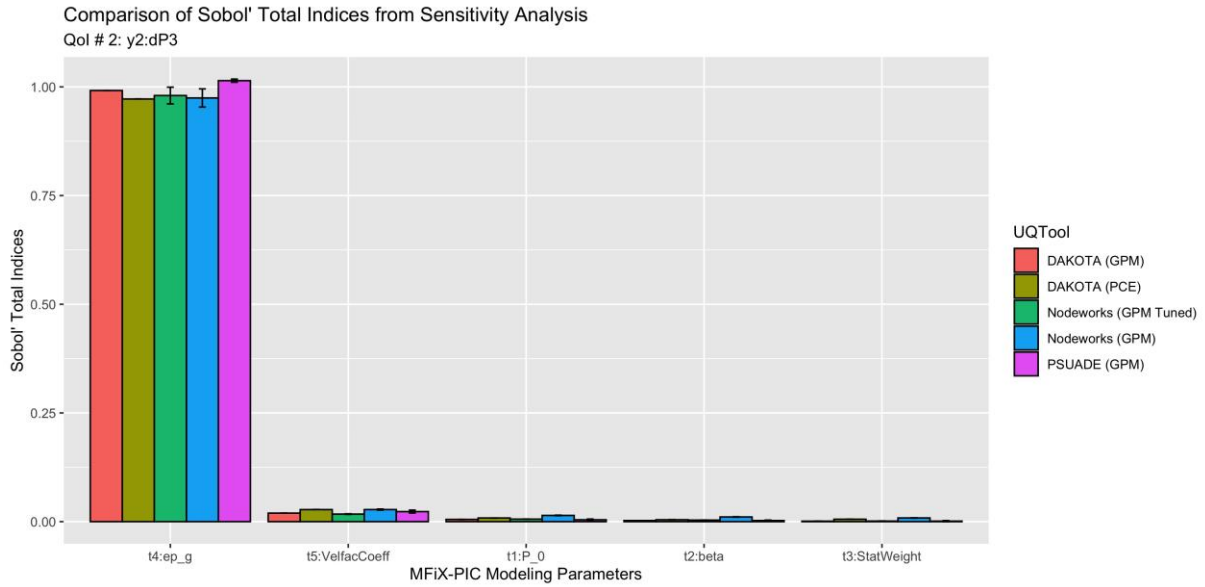

Figure 24: Comparison of Sobol' Total Indices for $y_2 : \Delta P_3$ based on the results from Nodeworks, PSUADE, and DAKOTA with the same input deck provided for Case 2 QoI # 2.

Figure 25 shows the Sobol' Total Indices for the third QoI, $y_3 : \Delta P_4$. Although $t4$:ep_g* appears to be the most influential similar to the previous two QoIs, the second ranking parameter appears to have changed from $t5$:VelFacCoeff to $t2$:beta, immediately followed by $t1$:P_0 as the third most influential parameter, which is different than the findings for the previous two QoIs. $y_3 : \Delta P_4$ as it includes a combination of dense bed and freeboard. Parcels transitioning between these regions are influenced by parameters besides just the void fraction at maximum packing. Significant sensitivities were observed to $t1$ and $t2$, though the exact reason is not known.

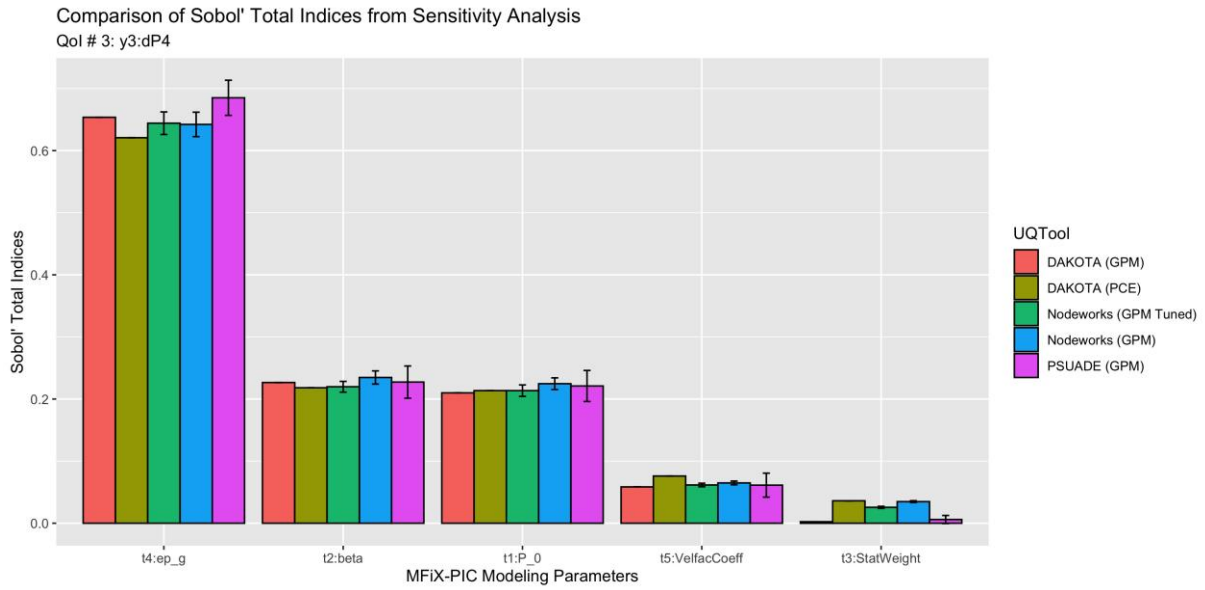

Figure 25: Comparison of Sobol' Total Indices for $y_3 : \Delta P_4$ based on the results from Nodeworks, PSUADE, and DAKOTA with the same input deck provided for Case 2 QoI # 3.

For all three QoIs, Nodeworks results show consistent order of importance ranking compared to DAKOTA and PSUADE.

5.4 CASE 3: CIRCULATING FLUIDIZED BED

Figure 26 shows the Sobol' Total Sensitivity Indices results for the first QoI in Case 3, i.e., y_1:Interface height in standpipe. The most influential parameter is identified as $t3$:StatWeight, which is followed by $t5$:VelFacCoeff and $t4$:ep_g* as the second and third, respectively.

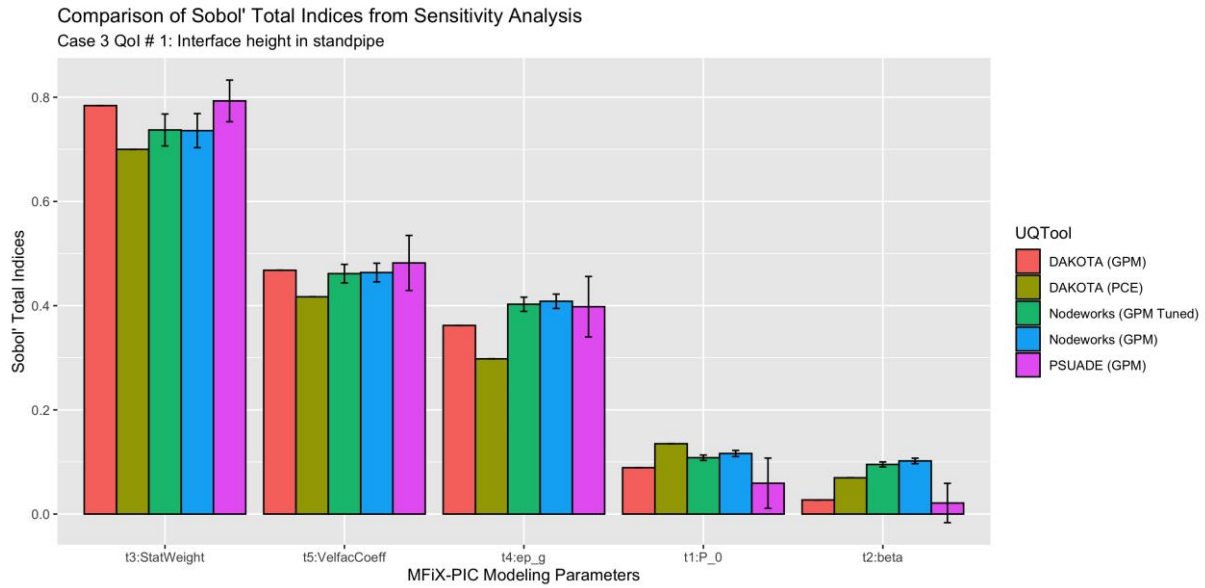

Figure 26: Comparison of Sobol' Total Indices for Case 3 QoI # 1 (y1: Interface height in standpipe) based on the results from Nodeworks, PSUADE, and DAKOTA with the same input deck provided.

Figure 27 shows the Sobol' Total Indices for the second QoI, y_2:Pressure drop across riser. For this QoI, the most influential input parameter was identified as $t3$:StatWeight. $t4$:ep_g* and $t5$:VelFacCoeff were identified as the second and third most influential parameters, respectively.

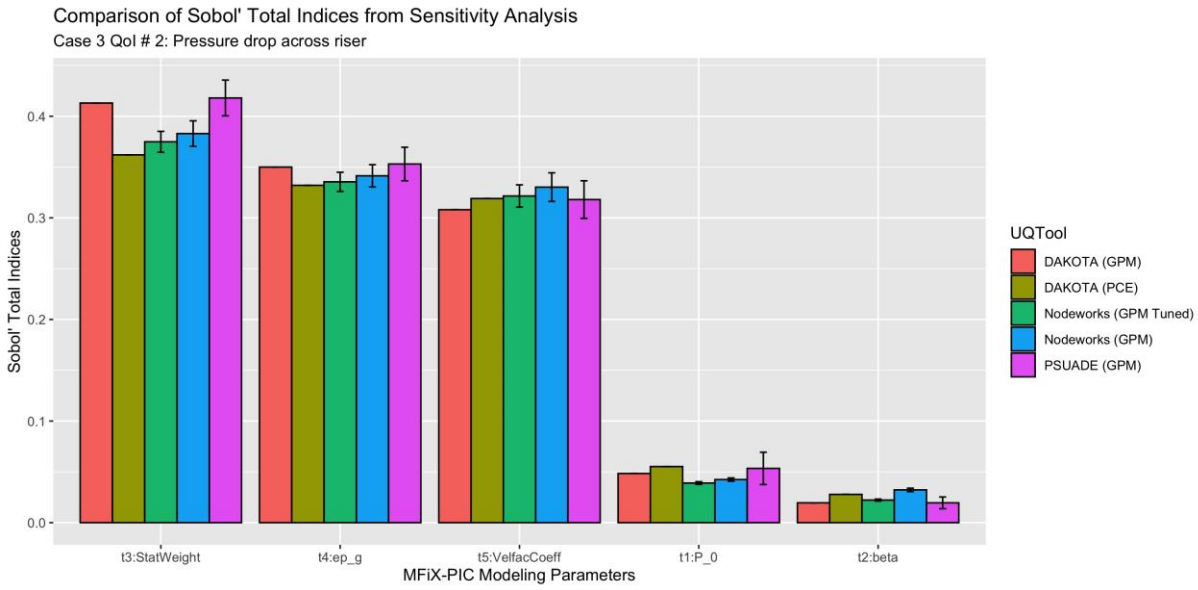

Figure 27: Comparison of Sobol' Total Indices for Case 3 QoI # 2 (y2: Pressure drop across riser) based on the results from Nodeworks, PSUADE, and DAKOTA with the same input deck provided.

Figure 28 shows the Sobol' Total Indices for the second QoI, y_3:Pressure drop across standpipe.

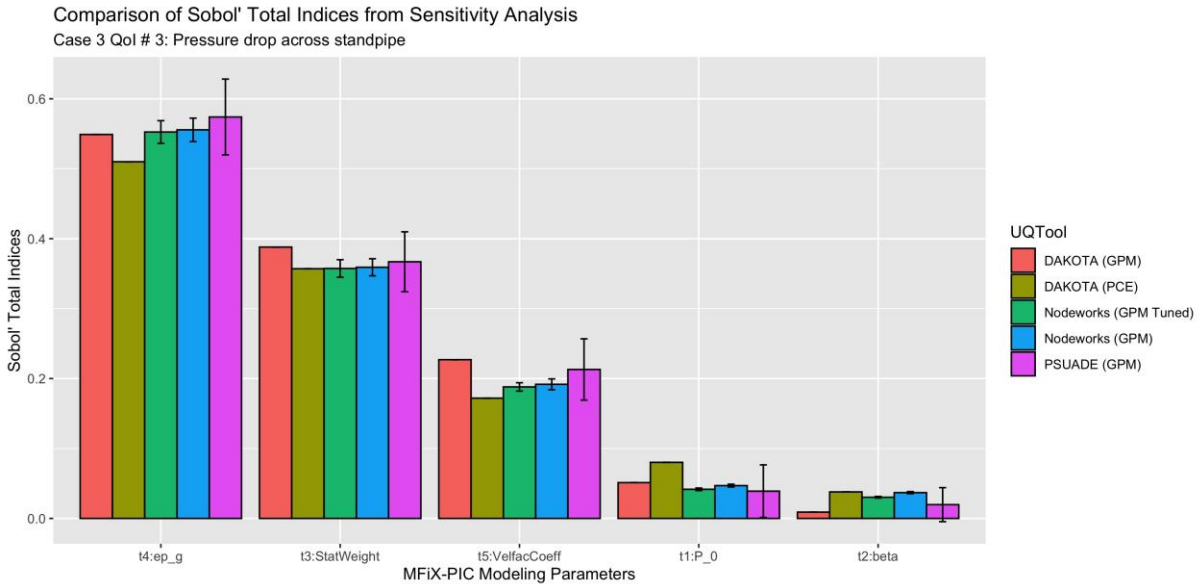

Figure 28: Comparison of Sobol' Total Indices for Case 3 QoI # 3 (y3: Pressure drop across standpipe) based on the results from Nodeworks, PSUADE, and DAKOTA with the same input deck provided.

For all three QoIs, Nodeworks results show consistent order of importance ranking compared to DAKOTA and PSUADE.

6. CONCLUSIONS

The work presented in this report was motivated by the need to assess if the UQ capabilities offered through Nodeworks operated as intended for a complete end-to-end UQ analysis workflow. Nodeworks consists of different Python libraries specialized on various aspects of the UQ analysis tasks, which come as standalone packages. The assessment was performed as a solution verification by comparing against the results of global sensitivity analysis obtained with the two other well-established UQ software, PSUADE and DAKOTA. It is important to emphasize that the objective was not to identify the best UQ software for a given analysis task but to compare the results from Nodeworks with the other two to assess if consistent results can be achieved when the same input, which was constructed from the simulation campaign results, is provided to all to perform the same UQ analysis.

Three distinct multiphase flow problems of interest were selected to carry out the same comparison. First case was a gravitational settling bed configuration, which was a unique problem as it also offered an analytical solution to perform precise error analysis to compare MFiX-PIC simulation results. Second and third cases were a laboratory scale bubbling fluidized bed configuration and laboratory scale circulating fluidized bed setup, respectively.

An initial comparison of the surrogate model construction in the three UQ software was performed for all cases. To construct a surrogate model, the results from the MFiX-PIC simulation campaign with 110 sampling locations (based on Latin Hypercube sampling) were used. The aim was to use the surrogate model to cheaply calculate the QoIs for the prescribed range of the selected input parameters, which is utilized during UQ analysis. Ten unseen sampling locations were then used to compare the predictions from surrogate models of the three UQ software. The predicted values were exactly the same (up to eight decimal places) while using a third-order polynomial based surrogate model. When GPM was used, notable differences were present, which were minimized by hyperparameter tuning in Nodeworks, though not completely eliminated. This may be attributed to differences in the implementation of GPMs in the UQ software tools used in this study.

This was followed by a global sensitivity analysis. Specifically, Sobol' Sensitivity Indices method was employed in each UQ software for verification of importance ranking. QoIs from simulation campaigns of three different cases were provided as input to the three UQ tools. GPM based surrogate models were constructed for each case (and each QoI). Subsequently, Sobol' Total Sensitivity Indices were estimated. Depending on flow physics, the ranking among MFiX-PIC model parameters changed. However, the importance ranking from Nodeworks was consistent with PSUADE and DAKOTA results. Even though this exercise used GPM primarily, the same level of consistency could be expected for the other types of surrogate models. It must be reiterated that the effort was aimed at assessing whether the same importance ranking can be obtained from Nodeworks by establishing a solution verification-based approach rather than an exhaustive study that aims to determine which UQ software is best for the analysis performed.

7. REFERENCES

Adams, B. M. The DAKOTA Toolkit for Parallel Optimization and Uncertainty Analysis; 2008.

Adams, B. M.; Bohnhoff, W. J.; Dalbey, K.; Eddy, J.; Eldred, M.; Gay, D.; Haskell, K.; Hough, P. D.; Swiler, L. P. *DAKOTA, a multilevel parallel object-oriented framework for design optimization, parameter estimation, uncertainty quantification, and sensitivity analysis: version 5.0 user's manual*; Tech. Rep. SAND2010-2183; Sandia National Laboratories, 2009.

Adams, B. M.; Hough, P. D. *DAKOTA Training: Advanced Topics*; 2012.

Adams, B. M.; Hough, P. D.; Swiler, L. P. *Dakota Software Training: Model Calibration*; 2015.

Gel, A.; Garg, R.; Tong, C.; Shahnam, M.; Guenther, C. Applying uncertainty quantification to multiphase flow computational fluid dynamics. *Powder Technology* **2013a,** *242*, 27–39.

Gel, A.; Li, T.; Gopalan, B.; Shahnam, M.; Syamlal, M. Validation and uncertainty quantification of a multiphase computational fluid dynamics model. *Industrial & Engineering Chemistry Research* **2013b,** *52*, 11424–11435.

Gel, A.; Shahnam, M.; Musser, J.; Subramaniyan, A. K.; Dietiker, J.-F. Nonintrusive uncertainty quantification of computational fluid dynamics simulations of a bench-scale fluidized-bed gasifier. *Industrial & Engineering Chemistry Research* **2016,** *55*, 12477–12490.

Gel, A.; Vaidheeswaran, A.; Clarke M. A. *Deterministic Calibration of MFiX-PIC, Part 1: Settling Bed*; DOE.NETL-2021.2646; NETL Technical Report Series; U.S. Department of Energy, National Energy Technology Laboratory: Morgantown, WV, 2021; p 72. DOI: 10.2172/1764832.

Geldart, D. Types of gas fluidization. *Powder Technology* **1973,** *7*, 285–292.

Iooss, B.; Lemaître, P. *Uncertainty management in simulation-optimization of complex systems*; Springer, 2015; pp 101–122.

Lin, G.; Engel, D. W.; Eslinger, P. W. Survey and evaluate uncertainty quantification methodologies; 2012.

NETL. MFIX Solver Suite Documentation. National Energy Technology Laboratory, https://mfix.netl.doe.gov/mfix/mfixdocumentation/ (accessed June 19, 2021).

NETL. Nodeworks User Guide - Response Surface Model Construction. National Energy Technology Laboratory, 2020a; https://mfix.netl.doe.gov/doc/nodeworks/20.2.0//userguide/sma/ rsm.html

NETL. Nodeworks. National Energy Technology Laboratory, 2020b; https://mfix.netl.doe.gov/nodeworks

Rasmussen, C.; Williams, C.; Press, M.; Bach, F.; (Firm), P. Gaussian Processes for Machine Learning; Adaptive computation and machine learning; MIT Press, 2006.

Simpson, T.; Toropov, V.; Balabanov, V.; Viana, F. Design and analysis of computer experiments in multidisciplinary design optimization: a review of how far we have come-or not. 12th AIAA/ISSMO Multidisciplinary Analysis and Optimization Conference, 2008; p 5802.

Sobol', I. M. Global sensitivity indices for nonlinear mathematical models and their Monte Carlo estimates. *Mathematics and computers in simulation* **2001,** *55*, 271–280.

Tong, C. Problem Solving Environment for Uncertainty Analysis and Design Exploration, Version 01., 2010; https://www.osti.gov//servlets/purl/1325009.

Tong, C. Problem Solving environment for Uncertainty Analysis and Design Exploration (PSUADE), 2020; https://computing.llnl.gov/projects/psuade/software.

Trucano, T. G.; Swiler, L. P.; Igusa, T.; Oberkampf, W. L.; Pilch, M. Calibration, validation, and sensitivity analysis: What's what. *Reliability Engineering & System Safety* **2006,** *91*, 1331–1357.

Vaidheeswaran, A.; Gel, A.; Clarke, M. A.; Rogers, W. A. *Sensitivity Analysis of Particle-In-Cell Modeling Parameters in Settling Bed, Bubbling Fluidized Bed and Circulating Fluidized Bed*; DOE.NETL-2021.2642; NETL Technical Report Series; U.S. Department of Energy, National Energy Technology Laboratory: Morgantown, WV, 2021; p 40. DOE: 10.2172/1756845.

Vaidheeswaran, A.; Li, C.; Ashfaq, H.; Wu, X.; Rowan, S.; Rogers, W. Data from experiments on bubbling fluidization of group B glass particles. *ChemRxiv*, 2020a.

Vaidheeswaran, A.; Musser, J.; Clarke, M. A. *Verification and Validation of MFiX-PIC*; NETL-TRS-2-2020; NETL Technical Report Series; U.S. Department of Energy, National Energy Technology Laboratory: Morgantown, WV, 2020b; p. 48. DOI: 10.2172/1618293.

Vaidheeswaran, A.; Rowan, S. Chaos and recurrence analyses of pressure signals from bubbling fluidized beds. *Chaos, Solitons & Fractals* **2020,** 110354.

Weber, J. Cyclone Optimization Using MFiX and Nodeworks, 2018. https://www.youtube.com/watch?v=40fNyuVLVlc.

Weber, J. Nodeworks Introduction, 2017. https://www.youtube.com/watch?v=taQVjBoCdF8.

Weber, J.; Fullmer, W.; Gel, A.; Musser, J. Optimization of a Cyclone Using Multiphase Flow Computational Fluid Dynamics. *Journal of Fluids Engineering* **2020,** *142*.

Williams, C. K.; Rasmussen, C. E. Gaussian processes for machine learning; MIT press Cambridge, MA, 2006; Vol. 2.

Xu, Y.; Musser, J.; Li, T.; Gopalan, B.; Panday, R.; Tucker, J.; Breault, G.; Clarke, M. A.; Rogers, W. A. Numerical simulation and experimental study of the gas–solid flow behavior inside a full-loop circulating fluidized bed: Evaluation of different drag models. *Industrial & Engineering Chemistry Research* **2018,** *57*, 740–750.

APPENDIX

The purpose of this Appendix is to provide information necessary for the reader to reproduce the results presented in this report for Nodeworks. There is expectation that the reader already has software access, as well as the necessary skill to work within and analyze results from associated software. The input files for PSUADE and DAKOTA were not included in the Gitlab repository as the primary objective of the appendix was to enable the reader to replicate the analysis presented with Nodeworks.

The files discussed in this section are available through NETL's Gitlab repository under the following URL:

https://mfix.netl.doe.gov/gitlab/quality-assurance/pic-sensitivity-study.git

The repository is publicly accessible at the time of the writing of this report.

Registered users can clone the repository for all PIC Sensitivity Study related studies with the following **git clone command** from a Linux console terminal, then navigate to the folder where Sensitivity Analysis related files reside:

```
1> git clone https://mfix.netl.doe.gov/gitlab/quality-assurance/pic-sensitivity-study.git
2> cd pic-sensitivity-study/
```

For those who use a GUI based Git client, users can point to https://mfix.netl.doe.gov/gitlab/quality-assurance/pic-sensitivity-study.git and clone the repository to their local system.

All files were tested on MacOS and Windows and are expected to be compatible with other operating system environments. If problems occur, the reader is encouraged to report them to the lead author via e-mail at aike@alpemi.com. Any other suggestions to improve the quality of the presented files and instructions in the appendix will be appreciated. For the corrections of errors discovered after the publication of this report, please visit the **Errata** folder in the Gitlab repository.

SIMULATION CAMPAIGN DATASETS

The results presented in this document and shared through Gitlab were based on MFiX-PIC version 20.1 simulations. The authors have become aware of a bug in MFiX-PIC solver that affects the results from simulation campaigns presented. As mentioned earlier, the objective of this work was to demonstrate and compare the sensitivity analysis with PSUADE, DAKOTA, and Nodeworks for any given input dataset (i.e., simulation campaign inputs and quantities of interest). Hence, no further revisions were implemented; however, the readers are warned about the potential differences should the reader use MFiX-PIC other than version 20.1 is to repeat the simulation campaigns.

The datafiles presented in this section are based on the compilation of the Optimal Latin Hypercube sampling-based design of experiments constructed for the five MFiX-PIC modeling input parameters in Comma Separated Values (CSV) formatted ASCII text files. The same set of input parameters (i.e., θ_1 : Pressure linear scale factor (P_0); θ_2 : Volume fraction exponential scale factor (β); θ_3 :Statistical Weight (W_p); θ_4 : Void fraction at maximal close packing$^{(\epsilon_g^*)}$; and

θ_5 : Solids slip velocity scale factor (α)) were used for each case but the lower and upper bounds were different for some of these parameters as shown in Tables 2, 3, and 4.

A.1 CASE 1: PARTICLE SETTLING

List of the file used with hyperlinks to the repository under "Simulation Campaign Datasets/Case1_ParticleSettling" folder:

C1_Fine_8July2020.csv : CSV formatted input dataset compiled including the results of the simulation campaign which contains five model input parameter settings and corresponding responses from MFiX-PIC simulations for the 110 sampling simulations. The QoIs are (i) y_1:Location of Settling Shock; (ii) y_2:Location of Filling Shock; (iii) y_3:Void fraction in the first cell nearest to the bottom of the experimental vessel.

List of the file used with hyperlinks to the repository under "Simulation Campaign Datasets/Case1_ParticleSettling/Nodeworks" folder:

EvalPt_wGPM_psuade_compare.nc : Nodeworks worksheet file, which contains all the nodes with the imported dataset to perform the construction of the surrogate model, sensitivity analysis using Sobol' Total Sensitivity Indices and the additional evaluations of the 10 samples used to compare the surrogate model predictions. The worksheet also demonstrates the case for untuned and hyperparameter tuned versions of the same workflow. A screenshot of the workflow constructed with this file is shown in Figure A1. The top two nodes in the figure (i.e., Response Surface Quad and Sensitivity Analysis node on the right) are for the surrogate model employing quadratic polynomial regression, and the resulting global sensitivity analysis ranking based on the quadratic regression surrogate model. The next three nodes shown (i.e., Response Surface, Sensitivity Analysis, and Parallel Coordinates Plot) are based on the Gaussian Process Model (GPM) based surrogate-model fitted and the sensitivity analysis results obtained from the untuned surrogate model. The Parallel Coordinates Plot on the right shows a visualization of the all of the simulation campaign datasets including both input parameters and QoI (i.e., y2=Location of Filling). The remaining Response Surface and Sensitivity Analysis nodes, which are labeled as Response Surface Tuned and Sensitivity Analysis Tuned, respectively are based on the hyperparameter tuned Gaussian Process Model surrogate model results. The other peripheral nodes are utilized to perform evaluations for the 10 unseen samples both by untuned and tuned surrogate models (i.e., Emulator nodes at the bottom), also output to file. The interested reader can review the worksheet and re-use its components for their own similar tasks.

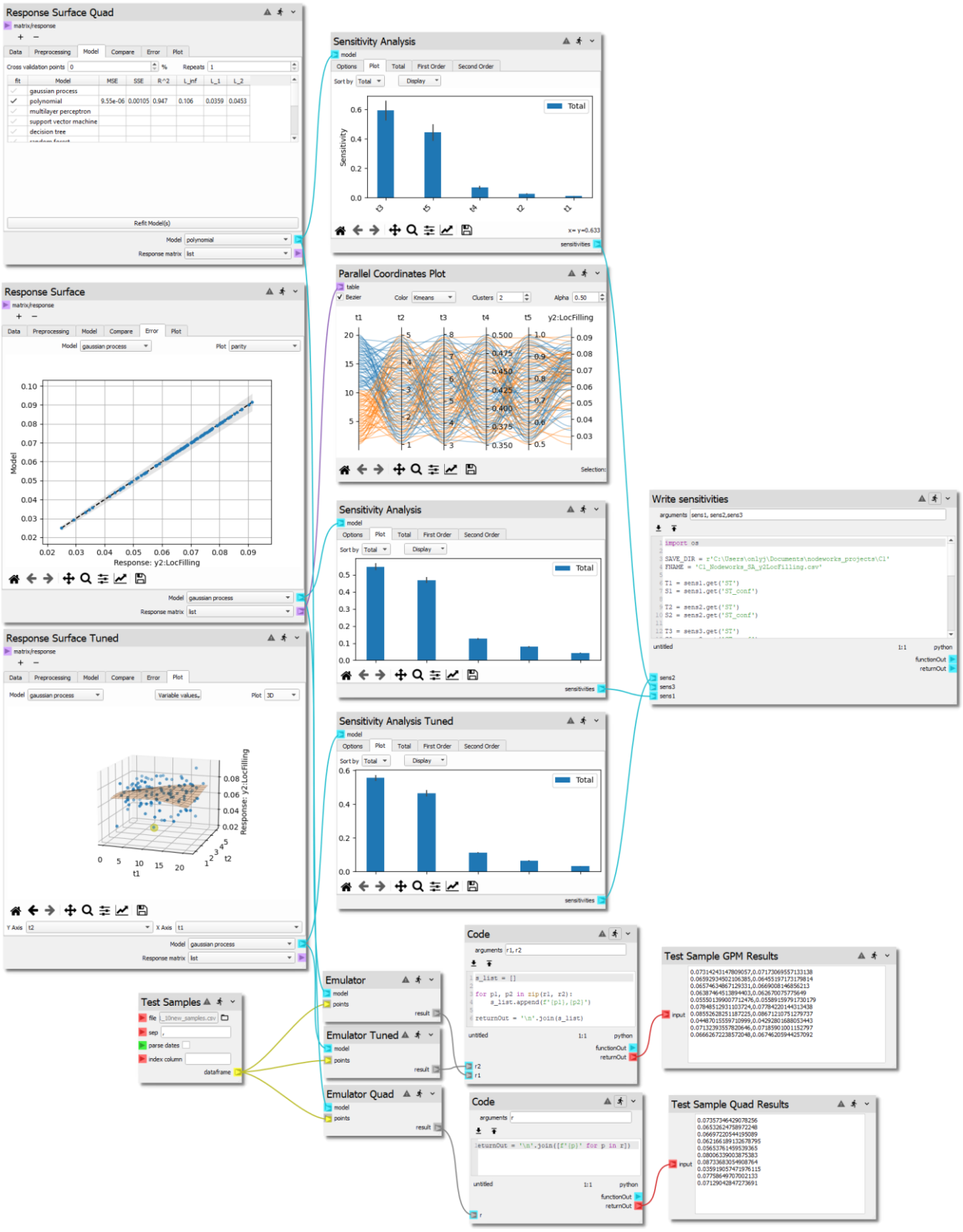

Figure A1: Screenshot of the Nodeworks workflow saved in EvalPt_wGPM_psuade_com-pare.nc.

Screenshot_C1_SA_y2FillLoc.png : The screenshot image of the workflow shown in Figure A1, which can be reviewed in Nodeworks by the reader by loading the EvalPt_wGPM_psuade_compare.nc worksheet file in the same folder.

List of the file used with hyperlinks to the repository under "Simulation Campaign Datasets/Case1_ParticleSettling/VerificationRuns" folder: C1_10new_samples.csv : The CSV formatted file for the 10 unseen sample points used as input to assess the Gaussian Process Model based surrogate model predictions and compare with respect to PSUADE an DAKOTA evaluations for the same set of input samples.

A.2 CASE 2: FLUIDIZATION

List of the file used with hyperlinks to the repository under "Simulation Campaign Datasets/Case2_Fluidization" folder:

C2_RSM_8May2020.csv : CSV formatted input dataset compiled including the results of the simulation campaign which contains five model input parameter settings and corresponding responses from MFiX-PIC simulations for the 110 sampling simulations. The QoIs are (i) $y1 : \Delta P_2$; (ii) $y2 : \Delta P_3$; (iii) $y3 : \Delta P_4$; (iv) $y4 : \Delta P_5$. Note that the last QoI ($y4$) was not considered in the analysis presented in this study.

List of the file used with hyperlinks to the repository under "Simulation Campaign Datasets/Case2_Fluidization/Nodeworks" folder:

C2_SA_y1dP2.nc : Nodeworks worksheet file for the first QoI (y1:dP2), which contains all the nodes with the imported dataset to perform the construction of the surrogate model, sensitivity analysis using Sobol' Total Sensitivity Indices and the additional evaluations of the 10 samples used to compare the surrogate model predictions.

C2_SA_y2dP3.nc : Nodeworks worksheet file for the second QoI (y2:dP3), which contains all the nodes with the imported dataset to perform the construction of the surrogate model, sensitivity analysis using Sobol' Total Sensitivity Indices and the additional evaluations of the 10 samples used to compare the surrogate model predictions.

C2_SA_y3dP4.nc : Nodeworks worksheet file for the third QoI (y3:dP4), which contains all the nodes with the imported dataset to perform the construction of the surrogate model, sensitivity analysis using Sobol' Total Sensitivity Indices and the additional evaluations of the 10 samples used to compare the surrogate model predictions.

List of the file used with hyperlinks to the repository under "Simulation Campaign Datasets/Case2_Fluidization/Verification Runs" folder:

C2_10new_samples.csv : The CSV formatted file for the 10 unseen sample points used as input to assess the Gaussian Process Model based surrogate model predictions and compare with respect to PSUADE an DAKOTA evaluations for the same set of input samples.

A.3 CASE 3: CFB

List of the file used with hyperlinks to the repository under "Simulation Campaign Datasets/Case3_CFB" folder:

C3_SA_Final.csv : CSV formatted input dataset compiled including the results of the simulation campaign which contains five model input parameter settings and corresponding responses from MFiX-PIC simulations for the 110 sampling simulations. The QoIs are (i) Interface height in standpipe (y_1:h_standpipe), (ii) Pressure drop across riser (y_2:dP_riser), and (iii) Pressure drop across standpipe (y_3:dP_standpipe).

List of the file used with hyperlinks to the repository under "Simulation Campaign Datasets/Case3_CFB/Nodeworks" folder:

C3_SA_y1.nc : Nodeworks worksheet file for the first QoI (y1: Interface height in standpipe), which contains all the nodes with the imported dataset to perform the construction of the surrogate model, sensitivity analysis using Sobol' Total Sensitivity Indices, and the additional evaluations of the 10 samples used to compare the surrogate model predictions.

C2_SA_y2.nc : Nodeworks worksheet file for the second QoI (y2: Pressure drop across riser), which contains all the nodes with the imported dataset to perform the construction of the surrogate model, sensitivity analysis using Sobol' Total Sensitivity Indices, and the additional evaluations of the 10 samples used to compare the surrogate model predictions.

C3_SA_y3.nc : Nodeworks worksheet file for the third QoI (y3: Pressure drop across standpipe), which contains all the nodes with the imported dataset to perform the construction of the surrogate model, sensitivity analysis using Sobol' Total Sensitivity Indices and the additional evaluations of the 10 samples used to compare the surrogate model predictions.

List of the file used with hyperlinks to the repository under "Simulation Campaign Datasets/Case3_CFB/Verification Runs" folder:

C3_10new_samples.csv : The CSV formatted file for the 10 unseen sample points used as input to assess the Gaussian Process Model based surrogate model predictions and compare with respect to PSUADE an DAKOTA evaluations for the same set of input samples.

This page intentionally left blank.

Brian Anderson
Director
National Energy Technology Laboratory
U.S. Department of Energy

Bryan Morreale
Executive Director
Research & Innovation Center
National Energy Technology Laboratory
U.S. Department of Energy

John Wimer
Associate Director
Strategic Planning
Science & Technology Strategic Plans
& Programs
National Energy Technology Laboratory
U.S. Department of Energy